A PRACTICAL GUIDE TO SCANNING PROBE MICROSCOPY

Authors (first edition) :
Rebecca Howland and Lisa Benatar

Project Editor and Booklet Designer: Christy Symanski
Copy Editor: Linda Emerson Technical Illustrator: Janet Okagaki

Revisions editor (March 2000): Jezz Leckenby
Production Coordinator and Cover Designer: Clarence Wong

CONTENTS I

INTRODUCTION

In the early 1980's scanning probe microscopes (SPMs) dazzled the world with the first real-space images of the surface of silicon. Now, SPMs are used in a wide variety of disciplines, including fundamental surface science, routine surface roughness analysis, and spectacular three-dimensional imaging—from atoms of silicon to micron-sized protrusions on the surface of a living cell.

The scanning probe microscope is an imaging tool with a vast dynamic range, spanning the realms of optical and electron microscopes. It's also a profiler with unprecedented 3-D resolution. In some cases, scanning probe microscopes can measure physical properties such as surface conductivity, static charge distribution, localized friction, magnetic fields, and elastic moduli. As a result, applications of SPMs are very diverse.

This booklet was written to help you learn about SPMs, a process that should begin with a thorough understanding of the basics. Issues covered in this booklet range from fundamental physics of SPMs to their practical capabilities and instrumentation. Examples of applications are included throughout the text, and several application-specific articles are listed at the end of each chapter.

ThermoMicroscopes was founded in 1998 with the merging of Park Scientific Instruments and TopoMetrix Corporation. Since the founding of these companies at the end of the 1980s, we have maintained strong ties to the academic community and a corporate philosophy that combines technology leadership with a practical-applications orientation. Our Analytical Services Laboratories work with customers to demonstrate the ability of our SPMs to meet their needs. We believe that the more you know about scanning probe microscopes, the more likely you'll be to choose our products. We want to provide you with the basic facts about SPMs before you make your way through sales literature—which tends to be more persuasive and less informative.

We hope you enjoy reading about this exciting technology. When you finish reading this booklet, please contact us. An order form for our sales literature is included at the back of the booklet. We'd also like to show you images from our image library, which spans a wide variety of applications.

CHAPTER 1
SPM TECHNIQUES

Scanning probe microscopes (SPMs) are a family of instruments used for studying surface properties of materials from the atomic to the micron level. All SPMs contain the components illustrated in Figure 1-1.

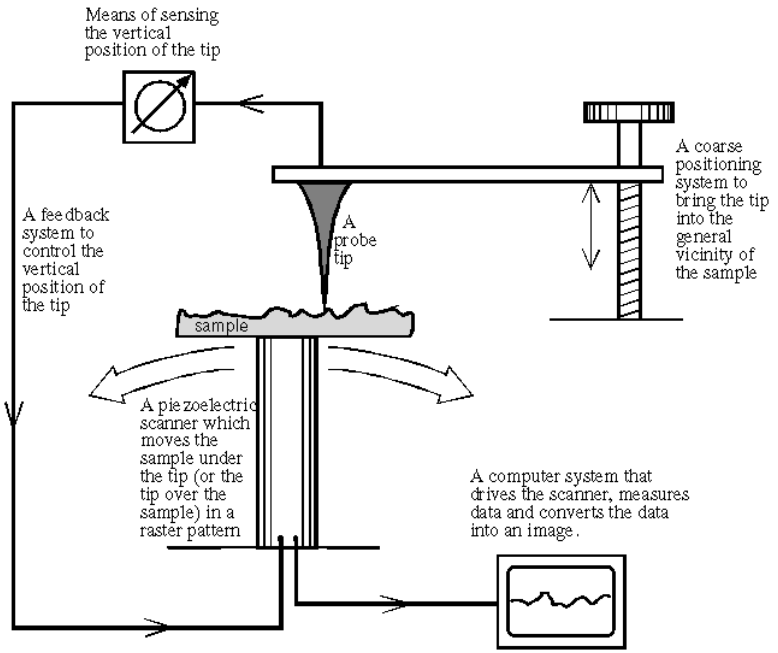

Figure 1-1. Schematic of a generalized SPM.

In this section, the operation of scanning tunneling microscopes (STMs), atomic force microscopes (AFMs), and other common scanning probe microscopes are discussed.

1.1 Scanning Tunneling Microscopy

The scanning tunneling microscope (STM) is the ancestor of all scanning probe microscopes. It was invented in 1981 by Gerd Binnig and Heinrich Rohrer at IBM Zurich. Five years later they were awarded the Nobel prize in physics for its invention. The STM was the first instrument to generate real-space images of surfaces with atomic resolution.

STMs use a sharpened, conducting tip with a bias voltage applied between the tip and the sample. When the tip is brought within about 10Å of the sample, electrons from the sample begin to "tunnel" through the 10Å gap into the tip or vice versa, depending upon the sign of the bias voltage. (See Figure 1-2.) The resulting tunneling current varies with tip-to-sample spacing, and it is the signal used to create an STM image. For tunneling to take place, both the sample and the tip must be conductors or semiconductors. Unlike AFMs, which are discussed in the next section, STMs cannot image insulating materials.

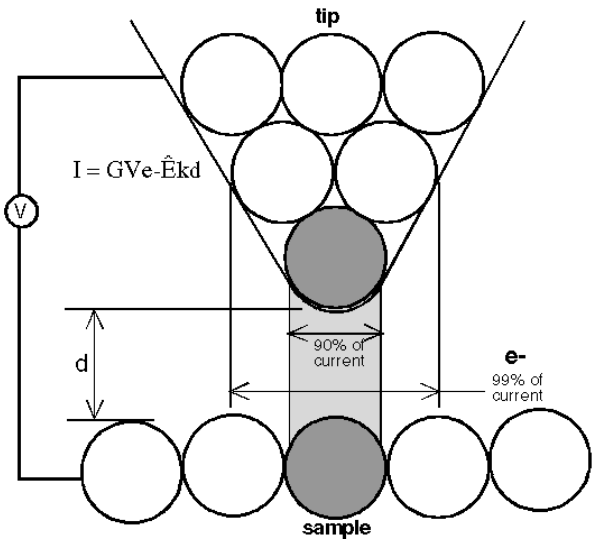

Figure 1-2. Schematic of tip and sample interaction for STM.

The tunneling current is an exponential function of distance; if the separation between the tip and the sample changes by 10% (on the order of 1Å), the

tunneling current changes by an order of magnitude. This exponential dependence gives STMs their remarkable sensitivity. STMs can image the surface of the sample with sub-angstrom precision vertically, and atomic resolution laterally.

STMs can be designed to scan a sample in either of two modes: *constant-height* or *constant-current* mode, as shown in Figure 1-3.

In constant-height mode, the tip travels in a horizontal plane above the sample and the tunneling current varies depending on topography and the local surface electronic properties of the sample. The tunneling current measured at each location on the sample surface constitute the data set, the topographic image.

In constant-current mode, STMs use feedback to keep the tunneling current constant by adjusting the height of the scanner at each measurement point. For example, when the system detects an increase in tunneling current, it adjusts the voltage applied to the piezoelectric scanner to increase the distance between the tip and the sample.

In constant-current mode, the motion of the scanner constitutes the data set. If the system keeps the tunneling current constant to within a few percent, the tip-to-sample distance will be constant to within a few hundredths of an angstrom.

Each mode has advantages and disadvantages. Constant-height mode is faster because the system doesn't have to move the scanner up and down, but it provides useful information only for relatively smooth surfaces. Constant-current mode can measure irregular surfaces with high precision, but the measurement takes more time.

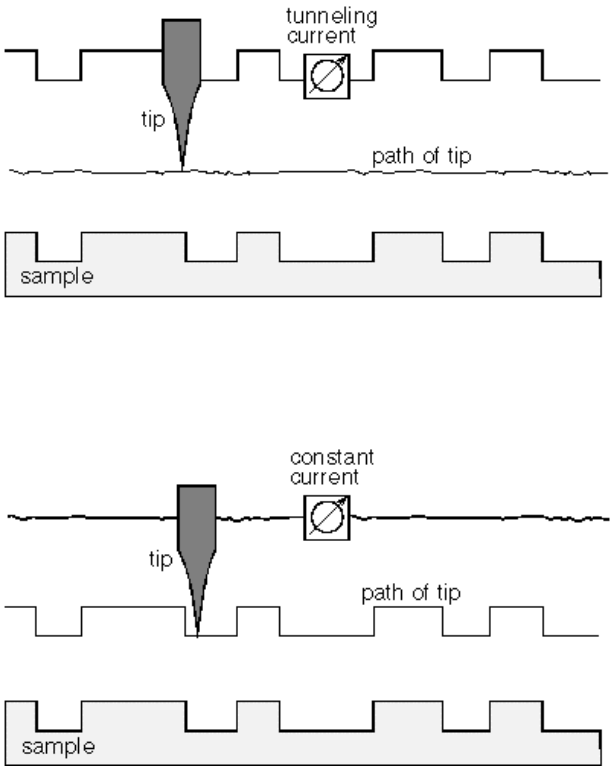

Figure 1-3. Comparison of constant-height and constant-current mode for STM.

As a first approximation, an image of the tunneling current maps the topography of the sample. More accurately, the tunneling current corresponds to the electronic density of states at the surface. STMs actually sense the number of filled or unfilled electron states near the Fermi surface, within an energy range determined by the bias voltage. Rather than measuring physical topography, it measures a surface of constant tunneling probability.

From a pessimist's viewpoint, the sensitivity of STMs to local electronic structure can cause trouble if you are interested in mapping topography. For example, if an area of the sample has oxidized, the tunneling current will drop precipitously when the tip encounters that area. In constant-current mode, the STM will instruct the tip to move closer to maintain the set tunneling current. The result may be that the tip digs a hole in the surface.

From an optimist's viewpoint, however, the sensitivity of STMs to electronic structure can be a tremendous advantage. Other techniques for obtaining information about the electronic properties of a sample detect and average the data originating from a relatively large area, a few microns to a few millimeters across. STMs can be used as surface analysis tools that probe the electronic properties of the sample surface with atomic resolution. Using STMs as spectroscopy tools is discussed in § 1.6.1, later in this chapter.

1.2 Atomic Force Microscopy

The atomic force microscope (AFM) probes the surface of a sample with a sharp tip, a couple of microns long and often less than 100Å in diameter. The tip is located at the free end of a cantilever that is 100 to 200µm long. Forces between the tip and the sample surface cause the cantilever to bend, or deflect. A detector measures the cantilever deflection as the tip is scanned over the sample, or the sample is scanned under the tip. The measured cantilever deflections allow a computer to generate a map of surface topography. AFMs can be used to study insulators and semiconductors as well as electrical conductors.

Several forces typically contribute to the deflection of an AFM cantilever. The force most commonly associated with atomic force microscopy is an interatomic force called the van der Waals force. The dependence of the van der Waals force upon the distance between the tip and the sample is shown in Figure 1-4.

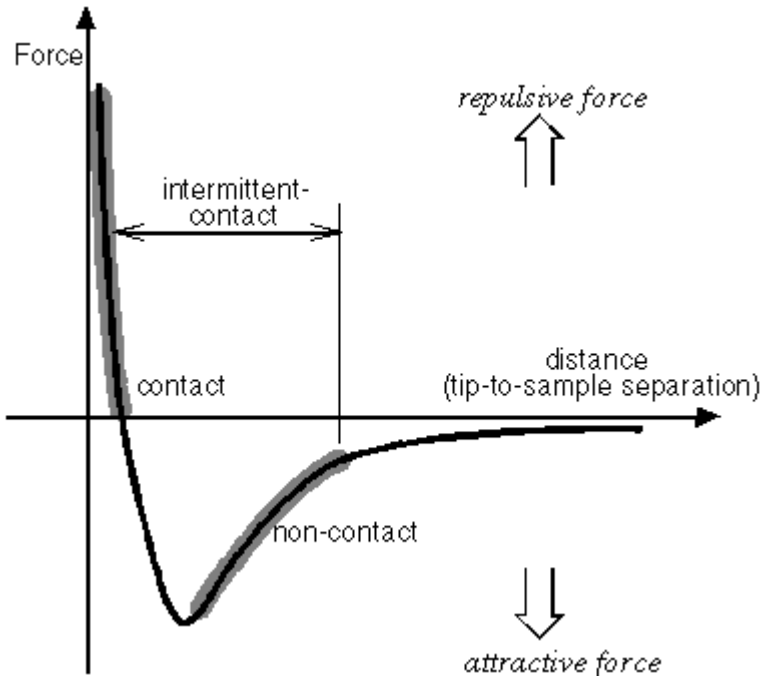

Figure 1-4. Interatomic force vs. distance curve.

Two distance regimes are labeled on Figure 1-4: 1) the contact regime; and 2) the non-contact regime. In the contact regime, the cantilever is held less than a few angstroms from the sample surface, and the interatomic force between the cantilever and the sample is repulsive. In the non-contact regime, the cantilever is held on the order of tens to hundreds of angstroms from the sample surface, and the interatomic force between the cantilever and sample is attractive (largely a result of the long-range van der Waals interactions). Both contact and non-contact imaging techniques are described in detail in the following sections.

1.2.1 Contact AFM

In contact-AFM mode, also known as repulsive mode, an AFM tip makes soft "physical contact" with the sample. The tip is attached to the end of a cantilever with a low spring constant, lower than the effective spring constant holding the atoms of the sample together. As the scanner gently traces the tip across the sample (or the sample under the tip), the contact force causes the cantilever to bend to accommodate changes in topography. To examine this scenario in more detail, refer to the van der Waals curve in Figure 1-4.

At the right side of the curve the atoms are separated by a large distance. As the atoms are gradually brought together, they first weakly attract each other. This attraction increases until the atoms are so close together that their electron clouds begin to repel each other electrostatically. This electrostatic repulsion progressively weakens the attractive force as the interatomic separation continues to decrease. The force goes to zero when the distance between the atoms reaches a couple of angstroms, about the length of a chemical bond. When the total van der Waals force becomes positive (repulsive), the atoms are in contact.

The slope of the van der Waals curve is very steep in the repulsive or contact regime. As a result, the repulsive van der Waals force balances almost any force that attempts to push the atoms closer together. In AFM this means that when the cantilever pushes the tip against the sample, the cantilever bends rather than forcing the tip atoms closer to the sample atoms. Even if you design a very stiff cantilever to exert large forces on the sample, the interatomic separation between the tip and sample atoms is unlikely to decrease much. Instead, the sample surface is likely to deform (see §1.5.7 on nanolithography).

In addition to the repulsive van der Waals force described above, two other forces are generally present during contact-AFM operation: a capillary force exerted by the thin water layer often present in an ambient environment, and the force exerted by the cantilever itself. The capillary force arises when water wicks its way around the tip, applying a strong attractive force (about 10^{-8}N) that holds the tip in contact with the surface. The magnitude of the capillary

force depends upon the tip-to-sample separation. The force exerted by the cantilever is like the force of a compressed spring. The magnitude and sign (repulsive or attractive) of the cantilever force depends upon the deflection of the cantilever and upon its spring constant. Section 1.6.2 examines these forces in more detail.

As long as the tip is in contact with the sample, the capillary force should be constant because the distance between the tip and the sample is virtually incompressible. It is also assumed that the water layer is reasonably homogeneous. The variable force in contact AFM is the force exerted by the cantilever. The total force that the tip exerts on the sample is the sum of the capillary plus cantilever forces, and must be balanced by the repulsive van der Waals force for contact AFM. The magnitude of the total force exerted on the sample varies from 10^{-8}N (with the cantilever pulling away from the sample almost as hard as the water is pulling down the tip—see §1.6.2), to the more typical operating range of 10^{-7} to 10^{-6}N.

Most AFMs currently on the market detect the position of the cantilever with optical techniques. In the most common scheme, shown in Figure 1-5, a laser beam bounces off the back of the cantilever onto a position-sensitive photodetector (PSPD). As the cantilever bends, the position of the laser beam on the detector shifts. The PSPD itself can measure displacements of light as small as 10Å. The ratio of the path length between the cantilever and the detector to the length of the cantilever itself produces a mechanical amplification. As a result, the system can detect sub-angstrom vertical movement of the cantilever tip.

Other methods of detecting cantilever deflection rely on optical interference, or even a scanning tunneling microscope tip to read the cantilever deflection. One particularly elegant technique is to fabricate the cantilever from a piezoresistive material so that its deflection can be detected electrically. (In piezoresistive materials, strain from mechanical deformation causes a change in the material's resistivity.) For piezoresistive detection, a laser beam and a PSPD are not necessary.

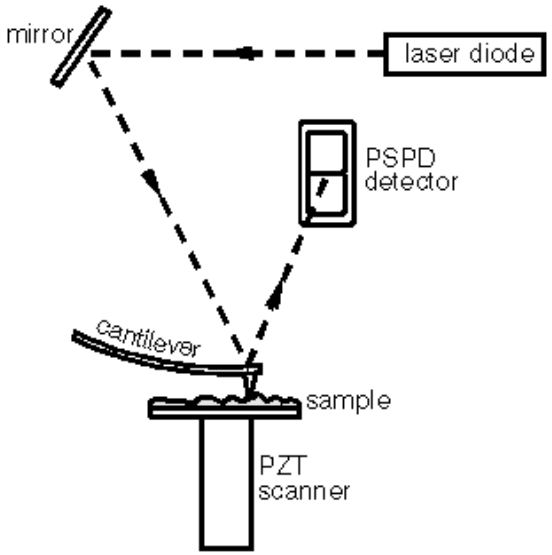

Figure 1-5. The beam-bounce detection scheme.

Once the AFM has detected the cantilever deflection, it can generate the topographic data set by operating in one of two modes- *constant-height* or *constant-force* mode.

In constant-height mode, the spatial variation of the cantilever deflection can be used directly to generate the topographic data set because the height of the scanner is fixed as it scans.

In constant-force mode, the deflection of the cantilever can be used as input to a feedback circuit that moves the scanner up and down in z, responding to the topography by keeping the cantilever deflection constant. In this case, the image is generated from the scanner's motion. With the cantilever deflection held constant, the total force applied to the sample is constant.

In constant-force mode, the speed of scanning is limited by the response time of the feedback circuit, but the total force exerted on the sample by the tip is well controlled. Constant-force mode is generally preferred for most applications.

Constant-height mode is often used for taking atomic-scale images of atomically flat surfaces, where the cantilever deflections and thus variations in applied force are small. Constant-height mode is also essential for recording real-time images of changing surfaces, where high scan speed is essential.

1.2.2 Non-contact AFM

Non-contact AFM (NC-AFM) is one of several vibrating cantilever techniques in which an AFM cantilever is vibrated near the surface of a sample. The spacing between the tip and the sample for NC-AFM is on the order of tens to hundreds of angstroms. This spacing is indicated on the van der Waals curve of Figure 1-4 as the non-contact regime.

NC-AFM is desirable because it provides a means for measuring sample topography with little or no contact between the tip and the sample. Like contact AFM, non-contact AFM can be used to measure the topography of insulators and semiconductors as well as electrical conductors. The total force between the tip and the sample in the non-contact regime is very low, generally about 10^{-12}N. This low force is advantageous for studying soft or elastic samples. A further advantage is that samples like silicon wafers are not contaminated through contact with the tip.

Because the force between the tip and the sample in the non-contact regime is low, it is more difficult to measure than the force in the contact regime, which can be several orders of magnitude greater. In addition, cantilevers used for NC-AFM must be stiffer than those used for contact AFM because soft cantilevers can be pulled into contact with the sample surface. The small force values in the non-contact regime and the greater stiffness of the cantilevers used for NC-AFM are both factors that make the NC-AFM signal small, and therefore difficult to measure. Thus, a sensitive, AC detection scheme is used for NC-AFM operation.

In non-contact mode, the system vibrates a stiff cantilever near its resonant frequency (typically from 100 to 400 kHz) with an amplitude of a few tens to hundreds of angstroms. Then, it detects changes in the resonant frequency or vibration amplitude as the tip comes near the sample surface. The sensitivity of this detection scheme provides sub-angstrom vertical resolution in the image, as with contact AFM.

The relationship between the resonant frequency of the cantilever and variations in sample topography can be explained as follows. The resonant frequency of a cantilever varies as the square root of its spring constant. In addition, the spring constant of the cantilever varies with the force gradient experienced by the cantilever. Finally, the force gradient, which is the derivative of the force versus distance curve shown in Figure 1-4, changes with tip-to-sample separation. Thus, changes in the resonant frequency of the cantilever can be used as a measure of changes in the force gradient, which reflect changes in the tip-to-sample spacing, or sample topography.

In NC-AFM mode, the system monitors the resonant frequency or vibrational amplitude of the cantilever and keeps it constant with the aid of a feedback system that moves the scanner up and down. By keeping the resonant frequency or amplitude constant, the system also keeps the average tip-to-sample distance constant. As with contact AFM (in constant-force mode), the motion of the scanner is used to generate the data set.

NC-AFM does not suffer from the tip or sample degradation effects that are sometimes observed after taking numerous scans with contact AFM. As mentioned above, NC-AFM is also preferable to contact AFM for measuring soft samples. In the case of rigid samples, contact and non-contact images may look the same. However, if a few monolayers of condensed water are lying on the surface of a rigid sample, for instance, the images may look quite different. An AFM operating in contact mode will penetrate the liquid layer to image the underlying surface, whereas in non-contact mode an AFM will image the surface of the liquid layer (see Figure 1-6).

For cases where a sample of low moduli may be damaged by the dragging of an AFM tip across its surface, another mode of AFM operation is available: intermittent-contact mode. Intermittent-contact mode is useful for a variety of applications, and it is described in the following section.

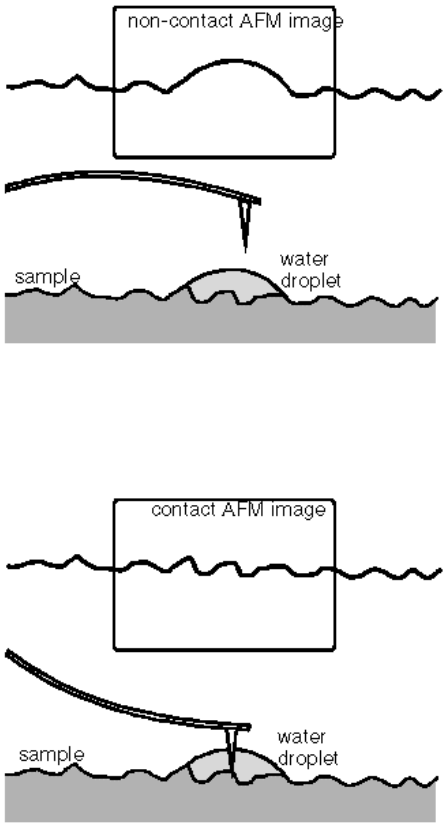

Figure 1-6. Contact and non-contact AFM images of a surface with a droplet of water.

1.2.3 Intermittent-contact AFM

Intermittent-contact atomic force microscopy (IC-AFM) is similar to NC-AFM, except that for IC-AFM the vibrating cantilever tip is brought closer to the sample so that at the bottom of its travel it just barely hits, or "taps," the sample. The IC-AFM operating region is indicated on the van der Waals curve in Figure 1-4. As for NC-AFM, for IC-AFM the cantilever's oscillation amplitude changes in response to tip-to-sample spacing. An image representing surface topography is obtained by monitoring these changes.

Some samples are best handled using IC-AFM instead of contact or non-contact AFM. IC-AFM is less likely to damage the sample than contact AFM because it eliminates lateral forces (friction or drag) between the tip and the sample. In general, it has been found that IC-AFM is more effective than NC-AFM for imaging larger scan sizes that may include greater variation in sample topography. IC-AFM has become an important AFM technique since it overcomes some of the limitations of both contact and non-contact AFM.

1.3 Magnetic Force Microscopy

Magnetic force microscopy (MFM) images the spatial variation of magnetic forces on a sample surface. For MFM, the tip is coated with a ferromagnetic thin film. The system operates in non-contact mode, detecting changes in the resonant frequency of the cantilever induced by the magnetic field's dependence on tip-to-sample separation. (See Figure 1-7.) MFM can be used to image naturally occurring and deliberately written domain structures in magnetic materials.

An image taken with a magnetic tip contains information about both the topography and the magnetic properties of a surface. Which effect dominates depends upon the distance of the tip from the surface, because the interatomic magnetic force persists for greater tip-to-sample separations than the van der Waals force. If the tip is close to the surface, in the region where standard non-contact AFM is operated, the image will be predominantly topographic. As you increase the separation between the tip and the sample, magnetic effects become apparent. Collecting a series of images at different tip heights is one way to separate magnetic from topographic effects.

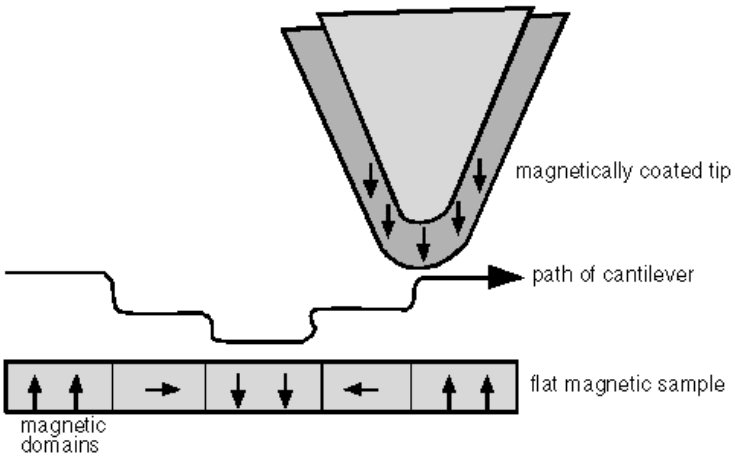

Figure 1-7. MFM maps the magnetic domains of the sample surface.

An image of a hard disk acquired in MFM mode is shown in Figure 1-8.

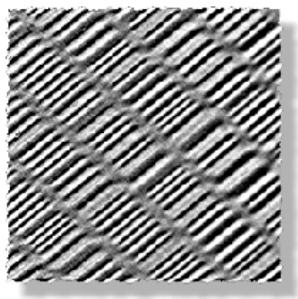

Figure 1-8. MFM image showing the bits of a hard disk. Field of view 30μm.

1.4 Lateral Force Microscopy

Lateral force microscopy (LFM) measures lateral deflections (twisting) of the cantilever that arise from forces on the cantilever parallel to the plane of the sample surface. LFM studies are useful for imaging variations in surface friction that can arise from inhomogeneity in surface material, and also for obtaining edge-enhanced images of any surface.

As depicted in Figure 1-9, lateral deflections of the cantilever usually arise from two sources: changes in surface friction and changes in slope. In the first case, the tip may experience greater friction as it traverses some areas, causing the cantilever to twist more strongly. In the second case, the cantilever may twist when it encounters a steep slope. To separate one effect from the other, LFM and AFM images should be collected simultaneously.

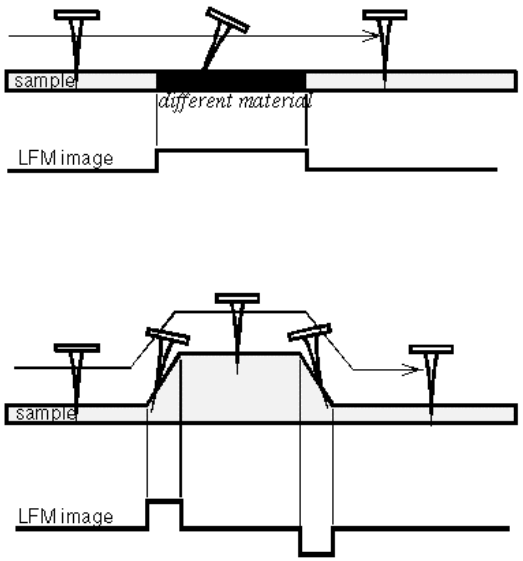

Figure 1-9. Lateral deflection of the cantilever from changes in surface friction (top) and from changes in slope (bottom).

LFM uses a position-sensitive photodetector to detect the deflection of the cantilever, just as for AFM. The difference is that for LFM, the PSPD also

senses the cantilever's twist, or lateral deflection. Figure 1-10 illustrates the difference between an AFM measurement of the *vertical* deflection of the cantilever, and an LFM measurement of *lateral* deflection. AFM uses a "bi-cell" PSPD, divided into two halves, A and B. LFM requires a "quad-cell" PSPD, divided into four quadrants, A through D. By adding the signals from the A and B quadrants, and comparing the result to the sum from the C and D quadrants, the quad-cell can also sense the lateral component of the cantilever's deflection. A properly engineered system can generate both AFM and LFM data simultaneously.

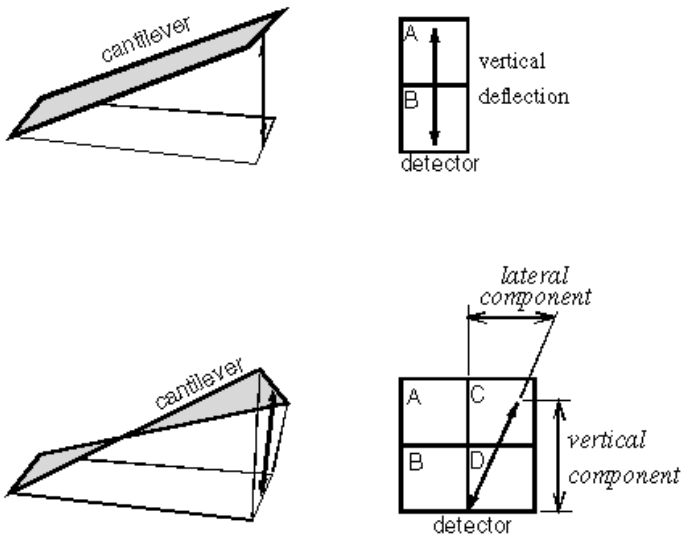

Figure 1-10. The PSPD for AFM (top) and LFM (bottom).

1.5 Other SPM Techniques

STM, contact, non-contact, and intermittent-contact AFM, MFM, and LFM are among the most common SPM techniques in practice today. Most commercial instruments are designed so that once you have purchased a basic unit, only small pieces of hardware have to be changed to provide different techniques. Sometimes, the only change required is switching from one mode to another mode using software. This section describes some of the additional techniques that are available.

1.5.1 Force Modulation Microscopy

Force modulation microscopy (FMM) is an extension of AFM imaging that includes characterization of a sample's mechanical properties. Like LFM and MFM, FMM allows simultaneous acquisition of both topographic and material-properties data.

In FMM mode, the AFM tip is scanned in contact with the sample, and the z feedback loop maintains a constant cantilever deflection (as for constant-force mode AFM). In addition, a periodic signal is applied to either the tip or the sample. The amplitude of cantilever modulation that results from this applied signal varies according to the elastic properties of the sample, as shown in Figure 1-11.

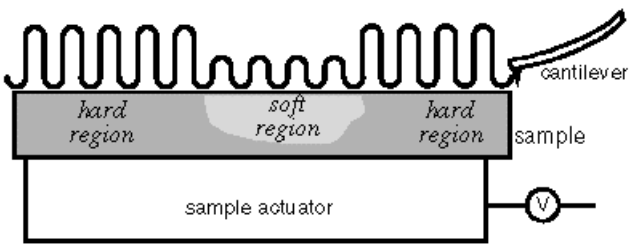

Figure 1-11. The amplitude of cantilever oscillation varies according to the mechanical properties of the sample surface.

The system generates a force modulation image, which is a map of the sample's elastic properties, from the changes in the amplitude of cantilever modulation. The frequency of the applied signal is on the order of hundreds of kilohertz, which is faster than the z feedback loop is set up to track. Thus, topographic information can be separated from local variations in the sample's elastic properties, and the two types of images can be collected simultaneously. Figure 1-12 shows a topographic contact-AFM image (left) and an FMM image (right) of a carbon fiber/polymer composite.

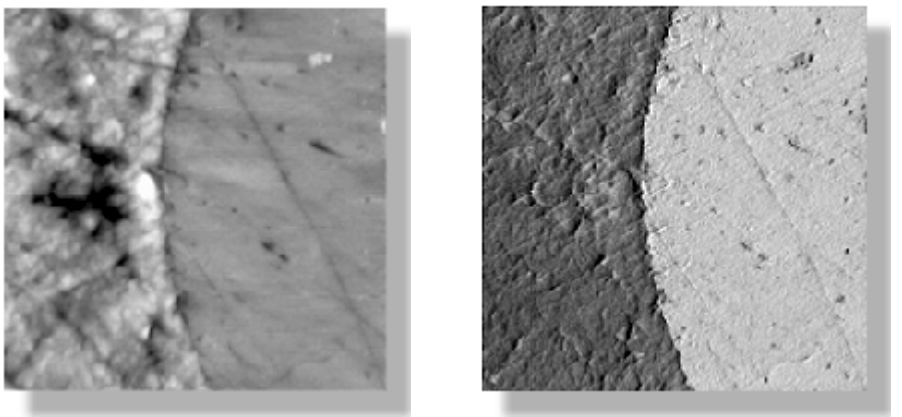

Figure 1-12. Contact-AFM (left) and FMM (right) images of a carbon fiber/polymer composite collected simultaneously. Field of view 5µm.

1.5.2 Phase Detection Microscopy

Phase detection microscopy (PDM)—also referred to as phase imaging—is another technique that can be used to map variations in surface properties such as elasticity, adhesion, and friction. Phase detection images can be produced while an instrument is operating in any vibrating cantilever mode, such as non-contact AFM, intermittent-contact AFM (IC-AFM), or MFM mode. Phase detection information can also be collected while a force modulation image (see §1.5.1) is being taken.

Phase detection refers to the monitoring of the phase lag between the signal that drives the cantilever to oscillate and the cantilever oscillation output signal. (See Figure 1-13.) Changes in the phase lag reflect changes in the mechanical properties of the sample surface.

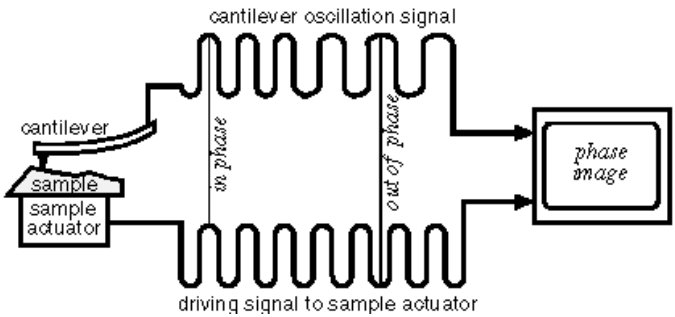

Figure 1-13. The phase lag varies in response to the mechanical properties of the sample surface.

The system's feedback loop operates in the usual manner, using changes in the cantilever's deflection or vibration amplitude to measure sample topography. The phase lag is monitored while the topographic image is being taken so that images of topography and material properties can be collected simultaneously.

One application of phase detection is to obtain material-properties information for samples whose topography is best measured using NC-AFM rather than contact AFM (see §1.2.3). For these samples, phase detection is useful as an alternative to force modulation microscopy, which uses contact AFM to measure topography.

Figure 1-14 shows a topographic non-contact AFM image (left) and a PDM image (right) of an adhesive label. The PDM image provides complementary information to the topography image, revealing the variations in the surface properties of the adhesive label.

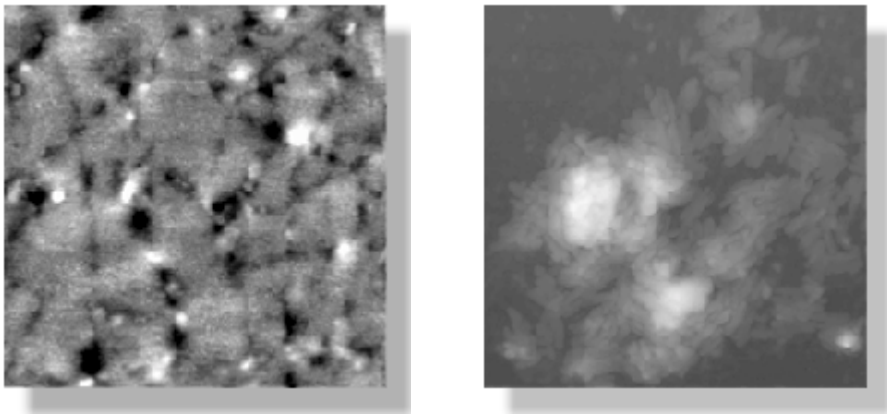

Figure 1-14. Non-contact AFM image (left) and PDM image (right) of an adhesive label, collected simultaneously. Field of view 3μm.

1.5.3 Electrostatic Force Microscopy

Electrostatic force microscopy (EFM) applies a voltage between the tip and the sample while the cantilever hovers above the surface, not touching it. The cantilever deflects when it scans over static charges, as depicted in Figure 1-15.

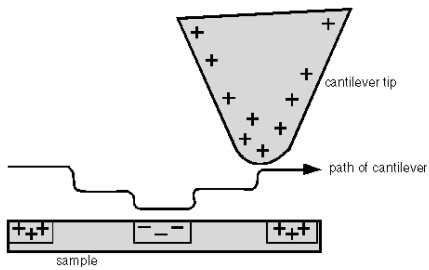

Figure 1-15. EFM maps locally charged domains on the sample surface.

EFM plots the locally charged domains of the sample surface, similar to how MFM plots the magnetic domains of the sample surface. The magnitude of the

deflection, proportional to the charge density, can be measured with the standard beam-bounce system. EFM is used to study the spatial variation of surface charge carrier density. For instance, EFM can map the electrostatic fields of a electronic circuit as the device is turned on and off. This technique is known as "voltage probing" and is a valuable tool for testing live microprocessor chips at the sub-micron scale.

1.5.4 Scanning Capacitance Microscopy

Scanning capacitance microscopy (SCM) images spatial variations in capacitance. Like EFM, SCM induces a voltage between the tip and the sample. The cantilever operates in non-contact, constant-height mode. A special circuit monitors the capacitance between the tip and the sample. Since the capacitance depends on the dielectric constant of the medium between the tip and the sample, SCM studies can image variations in the thickness of a dielectric material on a semiconductor substrate. SCM can also be used to visualize sub-surface charge-carrier distributions. For example, to map dopant profiles in ion-implanted semiconductors.

1.5.5 Scanning Thermal Microscopy

Scanning thermal microscopy (SThM) measures the thermal conductivity of the sample surface. Like MFM, LFM, and EFM, SThM allows simultaneous acquisition of both topographic and thermal conductivity data.

For SThM, there are different types of cantilever available. For example, a cantilever composed of two different metals is used. (Or, a thermal element made up of two metal wires can be used.) The materials of the cantilever respond differently to changes in thermal conductivity, and cause the cantilever to deflect. The system generates a SThM image, which is a map of the thermal conductivity, from the changes in the deflection of the cantilever. A topographic non-contact image can be generated from changes in the cantilever's amplitude of vibration. Thus, topographic information can be separated from local variations in the sample's thermal properties, and the two types of images can be collected simultaneously.

A second type of thermal cantilever uses a Wollaston wire as the probe. This incorporates a resistive thermal element at the end of the cantilever. The arms of the cantilever are made of silver wire. The resistive element at the end , which

forms the thermal probe is made from platinum or platinum/10% rhodium alloy. The advantage of this design is that it may be used in one of two modes allowing thermal imaging of sample temperature and thermal conductivity.

1.5.6 Near-field Scanning Optical Microscopy

NSOM is a scanning optical microscopy technique that enables users to work with standard optical tools beyond the diffraction limit that normally restricts the resolution capability of such methods. It works by exciting the sample with light passing through a sub-micron aperture formed at the end of a single-mode drawn optical fiber. Typically, the aperture is a few tens of nanometers in diameter. The fiber is coatd with aluminum to prevent light loss, thus ensuring a focused beam from the tip.

In a typical NSOM experiment, the probe is held fixed while the sample is scanned employing the same piezo technology found in most commercial scanning probe microscopes. In a modern system, the tip-to-sample distance may be regulated by employing a tuning fork-based shear-force feedback. The use of tuning fork technology means there is no neeed for an additional feedback laser as was the case with earlier NSOM designs.

Tuning forks also improve the force sensitivity and greatly facilitate set-up. This provides the experimenter much more flexibility in choosing the light wavelength to be used for the measurement. This results in simultaneous but independent optical and topographic images of the sample.

It is important that only a very small portion of the sample is illuminated. This significantly reduces photobleaching. This helps clarifying the relationship between optical and topographic structure of the sample.

The most commonly chosen imaging mode is fluorescence, but there have been other examples including UV-visible, IR and Raman techniques. In addition to its remarkable imaging capabilities, chemical information can be obtained using near-field spectroscopy at resolutions better than 100nm.

1.5.7 Nanolithography

Normally an SPM is used to image a surface without damaging it in any way. However, either an AFM or STM can be used to modify the surface deliberately, by applying either excessive force with an AFM, or high-field pulses with an STM. Not only scientific literature, but also newspapers and magazines have shown examples of surfaces that have been modified atom by atom. This technique is known as nanolithography. Figure 1-16 shows a photoresistive surface that has been modified using this technique.

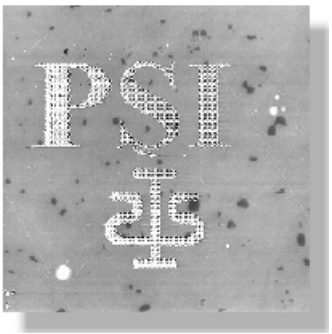

Figure 1-16. Image of a photoresistive surface that has been modified using nanolithography. Field of view 40μm.

1.5.8 Pulsed Force Mode

Pulsed Force Mode (PFM) employs an oscillating cantilever to probe a sample's surface and produces simultaneous but separate maps of sample topography, stiffness, and adhesion. In PFM, the probe scans the surface in contact mode feedback while a sinusoidal oscillation, well below the cantilever's resonant frequency, is applied to the z-piezo. This oscillation brings the tip into periodic contact with the surface as it scans the sample. This scan technique minimizes destructive lateral forces that may be induced by standard contact mode, and makes it possible to scan soft samples.

Through each oscillation, the system monitors probe displacement to characterize the force-distance relationship between the surface and the probe. This displacement is related to tip force by the spring constant of the cantilever. In order to minimize the data processing load, PFM measures only characteristic trigger points on the displacement curve. From these data points, are derived simultaneous topographic, stiffness and adhesion maps. Each contact becomes one pixel in the acquired image arrays. This data reduction method allows for much faster imaging rates than are possible with comparable techniques such as Layered Imaging™.

The sample topography image is generated by mapping the voltage changes that are applied to the z-piezo in order to keep the probe at a constant, maximum force (maximum probe deflection) at the end of each oscillation into the sample.

Stiffness is a primary mechanical characteristic, and gives an indication of the extent to which a material will deform under an applied force. PFM measures a sample's stiffness by calculating the average rate of probe deflection as the tip is oscillated into contact with the surface with increasing force. This measurement is taken over an arbitrary time interval prior to the maximum force.

The maximum tensile force that is observed during the retraction phase of the probe oscillation is used to determine the adhesion between the tip and sample. A sample with a strong adhesive interaction will hold the tip in contact as the cantilever attempts to pull it away from the surface. Thus a large force will be required in order to make the tip snap away from the surface. The PFM electronics will make a relative stiffness measurement based on the maximum cantilever deflection that occurs before the tip pulls free from the sample's surface.

PFM is an ideal technique for the analysis of multicomponant samples. Blended polymers and composites are examples of systems in which PFM's unique ability to acquire simultaneous stiffness and adhesion data in conjunction with a topography image allows the user to map physical properties that are frequently independent of the surface morphology.

1.5.9 Micro-Thermal Analysis

Surface visualisation and characterisation are combined in micro-thermal Analysis (µTA) which combines sub-micron thermal imaging (SThM) and localised calorimetric measurements. For these studies, the probe is made of Wollaston wire and acts as an active heat source (see 1.5.5). The probe resistance is proportional to the probe temperature. Changes in the current required to keep the probe at constant temperature produce a thermal conductivity map of the surface. Conversely, changes in the probe resistance as a constant current is applied generate local surface temperature maps. In addition, a temperature oscillation can be applied to the probe. The oscillation frequency is inversely proportional to the sub-surface penetration depth of the thermal wave. Hence, an image is simultaneously generated which contains information on thermal diffusivity and enables visualisation of sub-surface materials. Figure 2 shows the thermal conductivity variations in a carbon fibre composite material with high mechanical strength, used in the aviation industry. The fibres exhibit higher thermal conductivity relative to the surrounding epoxy matrix. The conductivity image clearly identifies the spatial distribution of the fibres in the cross-section sample.

The probe can additionally be placed at multiple points on the surface and localised thermal analysis performed. The temperature is ramped linearly and a sinusoidal temperature modulation is simultaneously applied. The power required to make the probe follow the temperature program provides a form of calorimetric measurement: micro-differential thermal analysis (µDTA). At the same time, the deflection of the probe is measured during heating recording the micro-thermomechanical analysis (µTMA) curve. Information on surface expansion, film thickness, glass transition temperatures, hardness changes, softening and melting processes can be determined from these plots.

The technology has been applied to a broad range of samples. Developed to gain a better understanding of polymers at the domain and interface levels, micro-thermal analysis has been shown to have applications to study pharmaceuticals (polymorphism and blending), paper (coatings) and aerospace materials (composites – matrix/fiber failure studies).

1.6 SPMs as Surface Analysis Tools

SPMs are most commonly thought of as tools for generating images of a sample's surface. SPMs can also be used, however, to measure material properties at a single x,y point on the sample's surface.

An STM can be used as a spectroscopy tool, probing the electronic properties of a material with atomic resolution. By comparison, the more traditional spectroscopies like XPS (x-ray photoelectron spectroscopy), UPS (ultra-violet photoelectron spectroscopy), or IPES (inverse photo-emission spectroscopy), detect and average the data originating from a relatively large area, a few microns to a few millimeters across. The study of the dependence of an STM signal upon the local electronic structure of the surface is known as scanning tunneling spectroscopy (STS).

The analogy for an AFM is the measurement of force vs. distance curves, which provide information about the local elastic properties of a surface. A force vs. distance curve is a plot of the force on an AFM cantilever tip in the z direction as a function of the z position of the piezoelectric scanner tube. STS and force vs. distance curves are discussed in the following sections.

1.6.1 Scanning Tunneling Spectroscopy

Scanning tunneling spectroscopy (STS) studies the local electronic structure of a sample's surface. The electronic structure of an atom depends upon its atomic species (whether it is a gallium atom or an arsenic atom, for instance) and also upon its local chemical environment (how many neighbors it has, what kind of atoms they are, and the symmetry of their distribution).

STS encompasses many methods: taking “topographic” (constant-current) images using different bias voltages and comparing them; taking current (constant-height) images at different heights; and ramping the bias voltage with the tip positioned over a feature of interest while recording the tunneling current. The last example results in current vs. voltage (I-V) curves characteristic of the electronic structure at a specific x,y location on the sample surface. STMs can be set up to collect I-V curves at every point in a data set, providing a three-dimensional map of electronic structure. With a lock-in amplifier, dI/dV (conductivity) or dI/dz (work function) vs. V curves can be collected

directly. All of these are ways of probing the local electronic structure of a surface using an STM.

1.6.2 Force vs. Distance Curves

Force vs. distance (F vs. d) curves are used to measure the vertical force that the tip applies to the surface while a contact-AFM image is being taken. This technique can also be used to analyze surface contaminants' viscosity, lubrication thickness, and local variations in the elastic properties of the surface.

Strictly speaking, a force vs. distance curve is a plot of the deflection of the cantilever versus the extension of the piezoelectric scanner, measured using a position-sensitive photodetector. The van der Waals force curve of Figure 1-4 represents just one contribution to the cantilever deflection. Local variations in the form of the F vs. d curve indicate variations in the local elastic properties. Contaminants and lubricants affect the measurement, as does the thin layer of water that is often present when operating an AFM in air.

In the laboratory, force vs. distance curves are quite complex and specific to the given system under study. The discussion here refers to Figure 1-17 and represents a gross simplification, where shapes, sizes, and distances should not be taken literally.

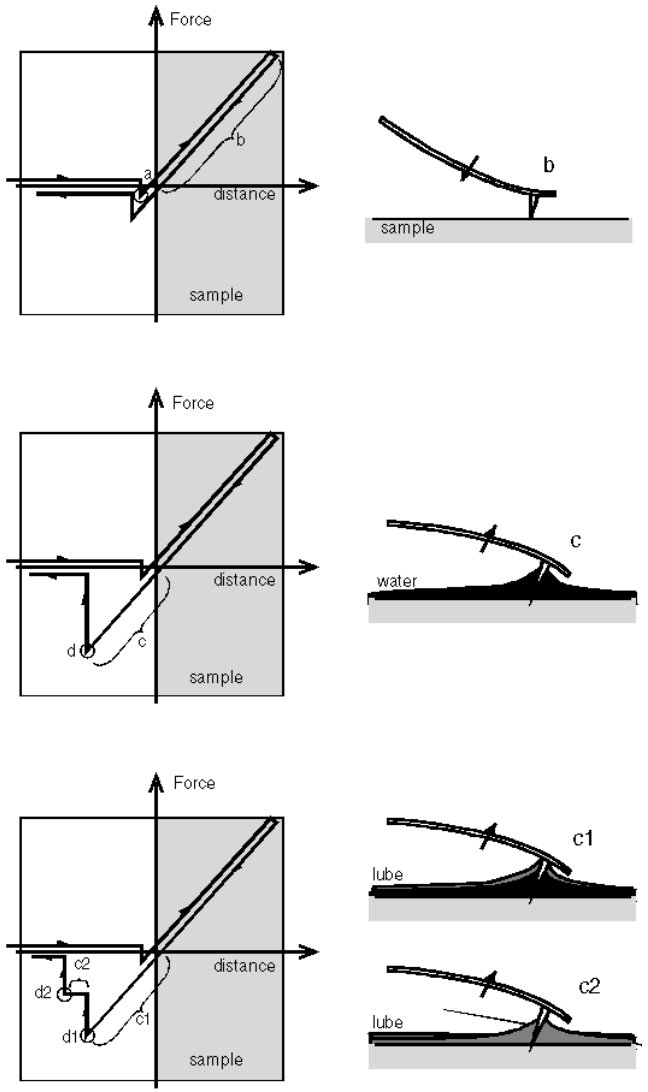

Figure 1-17. Forces vs. distance curves in vacuum (top), air (middle), and air with a contamination layer (bottom).

With this in mind, consider the simplest case of AFM in vacuum (Figure 1-17, top). At the left side of the curve, the scanner is fully retracted and the cantilever is undeflected since the tip is not touching the sample. As the scanner extends, the cantilever remains undeflected until it comes close enough to the sample surface for the tip to experience the attractive van der Waals force. The tip snaps into the surface (point **a** in Figure 1-17, top). Equivalently, the cantilever suddenly bends slightly towards the surface.

As the scanner continues to extend, the cantilever deflects away from the surface, approximately linearly (region **b** in Figure 1-17, top). After full extension, at the extreme right of the plot, the scanner begins to retract. The cantilever deflection retraces the same curve (in the absence of scanner hysteresis; see §2.2.2) as the scanner pulls the tip away from the surface.

In air, the retracting curve is often different because a monolayer or a few monolayers of water are present on many surfaces (Figure 1-17, middle). This water layer exerts a capillary force that is very strong and attractive. As the scanner pulls away from the surface, the water holds the tip in contact with the surface, bending the cantilever strongly towards the surface (region **c** in Figure 1-17, middle). At some point, depending upon the thickness of the water layer, the scanner retracts enough that the tip springs free (point **d** in Figure 1-17, middle). This is known as the snap-back point. As the scanner continues to retract beyond the snap-back point, the cantilever remains undeflected as the scanner moves it away from the surface in free space.

If a lubrication layer is present along with the water layer, multiple snap-back points can occur, as shown in Figure 1-17, bottom. The positions and amplitudes of the snap-back points depend upon the viscosity and thickness of the layers present on the surface.

Contact AFM can be operated anywhere along the linear portion of the force vs. distance curves, in regions (**b**) or (**c**). Operation in region (**c**) might be used for soft samples, to minimize the total force between the tip and the sample. Operating with the cantilever bent towards the surface is inherently a less stable situation, and maximum scan speeds may have to be reduced. Note that

operation in region (**c**) is still called contact mode, since the tip is touching the sample. Non-contact AFM is operated just to the left of point (**a**) on the F vs. d curve—just before the tip snaps into the surface.

In the linear region of the F vs. d curves (**b**), the slope is related to the elastic modulus of the system. When the cantilever is much softer than the sample surface, as is the case for non-destructive imaging, the slope of the curve mostly reflects the spring constant of the cantilever. However, when the cantilever is much stiffer than the sample surface, the slope of the F vs. d curve allows investigation of the elastic properties of the sample.

1.7 SPM Environments

Scanning probe microscopes can be operated in a variety of environments. In this section four environments are described: ultra-high vacuum (UHV), ambient (air), liquid, and electrochemical (EC).

1.7.1 Ultra-high Vacuum

The first STMs were operated primarily in UHV to study atomically clean surfaces. Silicon has been the most extensively studied material, and obtaining images of the 7 x 7 surface reconstruction of Si (111) is often used as a benchmark for evaluating the performance of UHV STM. A major application of UHV STM is scanning tunneling spectroscopy (see §1.6.1). STS applied to atomically clean surfaces allows characterization of both topographic and electronic structure, without the added complication of contamination that is always present in air. Another application is the study of materials processes in situ—that is, in the same vacuum environment in which the materials are grown. In this way, processing may proceed without contaminating the sample.

Although the first scanning probe microscope was a UHV STM, the development of UHV AFM came much later. Changing cantilevers and aligning the beam-bounce detection scheme—procedures that are not too difficult with an ambient AFM—were major obstacles to the development of a UHV AFM. However, the operation of both STM and AFM on the same vacuum flange is possible using piezoresistive cantilevers. A combined UHV STM/AFM enables scientists to work with conducting or non-conducting samples.

1.7.2 Ambient

The easiest, least expensive, and thus most popular environment for SPMs is ambient, or air. STM in air is difficult, since most surfaces develop a layer of oxides or other contaminants that interfere with the tunneling current. One class of materials for which ambient STM works well is layered compounds. In graphite, MoS_2, Nb_3Se, and so forth, a clean, "fresh" surface can be prepared by peeling away older surfaces. AFM is indifferent to sample conductivity, and thus can image any solid surface in air, including the contaminants.

1.7.3 Liquid

Liquid cells for the SPM allow operation with the tip and the sample fully submerged in liquid, providing the capability for imaging hydrated samples. Operation in liquid can also reduce the total force that the tip exerts on the sample, since the large capillary force (see §1.2.1) is isotropic in liquid.

A liquid environment is useful for a variety of SPM applications, including studies of biology, geologic systems, corrosion, or any surface study where a solid-liquid interface is involved. AFM, LFM, IC-AFM, FMM, and PDM images can be taken in a liquid environment. Figure 1-18 shows an IC-AFM image of rabbit muscle myofibril taken in liquid.

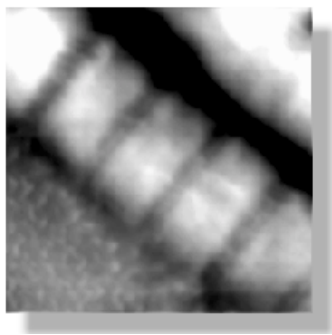

Figure 1-18. IC-AFM image of rabbit muscle myofibril taken in liquid. Field of view 7μm.

1.7.4 Electrochemical

Like UHV, electrochemical cells provide a controlled environment for SPM operation. Usually provided as an option for ambient SPMs, EC-SPMs consist of a cell, a potentiostat, and software. Applications of EC-SPM include real-space imaging of electronic and structural properties of electrodes, including changes induced by chemical and electrochemical processes, phase formation, adsorption, and corrosion as well as deposition of organic and biological molecules in electrolytic solution.

1.8 Further Reading

Sang-il Park and Robert C. Barrett, “Design Considerations for an STM System," Methods of Experimental Physics, vol. 27; Scanning Tunneling Microscopy, Ch. 2, pp. 31-76.

G.S. Blackman, C.M. Mate, and M.R. Philpott, “Interaction Forces of a Sharp Tungsten Tip with Molecular Films on Silicon Surfaces,” Physical Review Letters, vol. 65, No. 18.

Robert Pool, “The Children of the STM,” Science, vol. 247, pp. 643-636.

J.R. Matey and J. Blanc, “Scanning Capacitance Microscopy,” J. Appl. Phys. 57 (5), 1 March 1985, pp. 1437-1444.

P.K. Hansma, V.B. Elings, O. Marti, and C.E. Bracker, “Scanning Tunneling Microscopy and Atomic Force Microscopy: Application to Biology and Technology,” Science, vol. 242, 14 October 1988, pp. 209-216.

Y. Kuk and P.J. Silverman, “Scanning Tunneling Microscope Instrumentation,” Rev. Sci. Instrum. 60 (2), February 1989, pp. 165-181.

C. Mathew Mate, Max R. Lorenz, and V.J. Novotny, "Atomic Force Microscopy of Polymeric Liquid Films," J. Chem. Phys. 90 (12), 15 June 1989, pp. 7550-7555.

A.L. Weisenhorn, P.K. Hansma, T.R. Albrecht and C.F. Quate, “Forces in Atomic Force Microscopy in Air and Water,” Appl. Phys. Lett. 54 (26), 26 June 1989, pp. 2651-2653.

G.S. Blackman, C.M. Mate, and M.R. Philpott, “Atomic Force Microscope Studies of Lubricant Films on Solid Surfaces,” Surface Science, 31 August, 1989, pp. 1-13.

William A. Ducker, Robert F. Cook, and David R. Clarke, “Force Measurement Using an AC Atomic Force Microscope,” J. Appl. Phys. 67 (9), 1 May 1990, pp. 4045-4052.

Bharat Bhusan and G.S. Blackman, “Atomic Force Microscopy of Magnetic Rigid Disks and Sliders and Its Applications to Tribology,” Transactions of the ASME Journal of Tribology, 90-Trib-5, 1990, pp. 1-6.

G.S. Blackman, “Atomic Force Microscope Studies of Lubricant Films on Solid Surfaces,” Vacuum, vol. 41, No. 4-6, 1990, pp. 1283-1285.

Andrew Pollack, “Atom by Atom, Scientists Build ‘Invisible’ Machines of the Future,” The New York Times, 26 November 1991, B5, B7.

A.L. Weisenhorn, P. Maivald, H.J. Butt, and P.K. Hansma, “Measuring Adhesion, Attraction, and Repulsion between Surfaces in Liquids with an Atomic-Force Microscope,” Physical Review B, vol. 45, No. 19, 15 May 1992, pp. 11 226-11 232.

C. Mathew Mate, “Atomic-force-microscope Study of Polymer Lubricants on Silicon Surfaces,” Physical Review Letters, vol. 68, No. 22, 1 June 1992, pp. 3323-3326.

Jan H. Hoh, Jason P. Cleveland, Craig B. Prater, Jean-Paul Revel, and Paul K. Hansma, “Quantized Adhesion Detected with the Atomic Force Microscope,” J. Am. Chem. Soc., 1992, pp. 4917-4918.

John Markoff, “A Novel Microscope Probes the Ultra Small,” New York Times, February 23, 1993, C1, C8.

R.M. Penner, “Nanometer-Scale Synthesis and Atomic Scale Modification With the Scanning Tunneling Microscope," Scanning Microsc., 7, 1993, p. 805.

R. Fainchtein, S.T. D’Arcangelis, S.S. Yang, D.O. Cowan, S. Yoon, S. Pan, W.F. Smith, M. Yoo, A.L. de Lozanne, “Scanning Tunneling and Force Microscopies of Low-dimensional Organic Conductors and Superconductors,” Scanning Probe Microscopies, SPIE vol. 1855, 1993, pp. 129-139.

Jeffrey L. Hutter and John Bechhoefer, “Manipulation of Van der Waals Forces to Improve Image Resolution in Atomic Force Microscopy,” Journal of Applied Physics, vol. 73, 1993, pp. 4123-4129.

Jeffrey L. Hutter and John Bechhoefer, “Measurement and Manipulation of Van der Waals Forces in Atomic Force Microscopy,” Journal of Vacuum Science and Technology B, vol. 12, 1994, pp. 2251-2253.

G.S. Hsiao, R.M. Penner, and J. Kingsley, “Deposition of Metal Nanostructures onto Si(111) Surfaces by Field Evaporation in the Scanning Tunneling Microscope," Appl. Phys. Lett., 64, 1994, p. 1350.

J.A. Virtanen, S. Lee, W. Li, and R.M. Penner, “Measurement of the Localized Viscosity of Molecular Assemblies Using Nanoscopic Defects Induced with the Scanning Tunneling Microscope,” J. Phys. Chem., 98, 1994, p. 2663.

T.L. Porter, A.G. Sykes and G. Caple, “Scanning Probe Microscope Imaging of Polyaniline Thin Films in Non-Contact Mode, Surface and Interface Analysis,” 21, 1994, p. 814.

O. Yu. Nickolayev, V.F. Petrenko, “Study of Dislocations in ZnS and ZnSe by Scanning Force Microscopy,” J. Vac. Sci. and Technol., B12 (4), 1994, p. 2443.

A.N. Campbell, E.I. Cole Jr., B.A. Dodd, R.E. Anderson, “Magnetic Force Microscopy/Current Contrast Imaging: A New Technique for Internal Current Probing of ICs,” Microelectronic Engineering 24, 1994, pp. 11-22.

S. Gwo, K.J. Chao and C.K. Shih, “Cross-sectional Scanning Tunneling Microscopy of Doped and Undoped AlGaAs/GaAs Heterostructures," Appl. Phys. Lett. 64, 1994, p. 492.

F. Ho, A.S. Hou, and D.M. Bloom, "High-speed Integrated Circuit Probing Using A Scanning Force Microscope Sampler," Electronics Letters, vol. 30, no. 7, March 31, 1994, pp. 560-562.

T.L. Porter, D. Minore, R. Stein and M. Myrann, “Scanning Probe Microscope and Effective Medium Theory Study of Free-standing Polyaniline Thin Films,” J. Polymer Sci. 33, 1995, p. 2167.

T.M. McIntire, R.M. Penner, and D.A. Brant, Macromol., “Observations of a Circular, Triple-helical Polysaccharide Using Non-contact Atomic Force Microscopy," 28, 1995, p. 6375.

V. Shivshankar, D.J. Sandman, J. Kumar, S.K. Tripathy and C. Sung, ed. G.W. Bailey, M.H. Ellisman, R.A. Hennigar and N. J. Zaluzec “Investigation of Thermochromic Polydiacetylenes Using Atomic Force Microscopy," Microscopy and Microanalysis, Jones and Begell Publishing, NY, 1995, p. 490.

A.R. Smith, K.J. Chao, C.K. Shih, Y.C. Shih and B.G. Streetman, “Cross-sectional STM of AlAs/GaAs Short Period Superlattices: The Influence of Growth Interrupt on the Interfacial Structures," Appl. Phys. Lett. 66, 1995, p. 478.

F. Giessibl. "Atomic Resolution of the Silicon (1 1 1)-(7 x 7) Surface by Atomic Force Microscopy," Science, vol. 267, January 6, 1995, pp. 68-71.

B.A. Nechay, F. Ho, A.S. Hou, and D.M. Bloom, "Applications of an Atomic Force Microscope Voltage Probe with Ultrafast Time Resolution," J. Vac. Sci. Technol., May/June 1995, pp. 1369-1374.

O.L. Shaffer, R. Bagheri, J.Y. Qian, V. Dimonie, R.A. Pearson and M.S. El-Aasser, “Characterization of the Particle-matrix Interface in Rubber Modified Epoxy by Atomic Force Microscopy,” J. of Appl. Polymer Sci., vol. 58, No. 2, October 10, 1995, pp. 465-484.

V. Shivshankar, C. Sung, J. Kumar, S.K. Tripathy and D. J. Sandman, “Atomic Force Microscopy Studies of Diacetylene Monomers and Polymer," manuscript submitted to PMSE Abstracts for ACS National Meeting, New Orleans, LA, (March 1996).

A. Hammiche, H. M. Pollock, D.J. Hourston, M. Reading, & M Song (1996) Localised thermal analysis using a miniaturised resistive probe. *Rev Sci. Instrum.* **67** 4268-4274.

A. Hammiche, H. M. Pollock, M. Reading, M. Claybourn, P. H. Turner, and K. Jewkes (1999) Photothermal FTIR spectroscopy: a step towards FTIR microscopy at a resolution better than the diffraction limit. *Appl. Spectroscopy* **53** 810-815.

D. M. Price, M. Reading, A. Hammiche & H. M. Pollock (1999), Micro-thermal analysis: scanning thermal microscopy and localised thermal analysis. *Int. J. Pharmaceutics*, **191**(1), 97-103.

CHAPTER 2
THE SCANNER

In virtually all scanning probe microscopes, a piezoelectric scanner is used as an extremely fine positioning stage to move the probe over the sample (or the sample under the probe). The SPM electronics drive the scanner in a type of raster pattern, as shown in Figure 2-1.

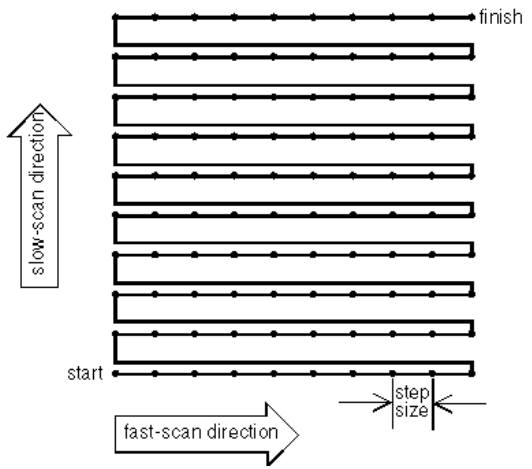

Figure 2-1. Scanner motion during data acquisition.

The scanner moves across the first line of the scan, and back. It then steps in the perpendicular direction to the second scan line, moves across it and back, then to the third line, and so forth. The path differs from a traditional raster pattern in that the alternating lines of data are not taken in opposite directions. SPM data are collected in only one direction—commonly called the fast-scan direction—to minimize line-to-line registration errors that result from scanner hysteresis (see §2.2.2). The perpendicular direction, in which the scanner steps from line to line, is called the slow-scan direction.

While the scanner is moving across a scan line, the image data are sampled digitally at equally spaced intervals. The data are the height of the scanner in z for constant-force mode (AFM) or constant-current mode (STM). For constant-height mode, the data are the cantilever deflection (AFM) or tunneling current (STM) (see §1.2.1 and §1.1).

The spacing between the data points is called the step size. The step size is determined by the full scan size and the number of data points per line. In a typical SPM, scan sizes run from tens of angstroms to over 100 microns, and from 64 to 512 data points per line. (Some systems offer 1024 data points per line.) The number of lines in a data set usually equals the number of points per line. Thus, the ideal data set is comprised of a dense, square grid of measurements.

The difficulties of achieving a perfectly square measurement grid in the plane of the sample surface are explored in this chapter. And similar difficulties arise in the perpendicular (z) direction. To gain an understanding of the mechanisms underlying scanner operation, the fundamentals of piezoelectric scanners are discussed.

2.1 Scanner Design and Operation

Piezoelectric materials are ceramics that change dimensions in response to an applied voltage. Conversely, they develop an electrical potential in response to mechanical pressure. Piezoelectric scanners can be designed to move in x, y, and z by expanding in some directions and contracting in others.

Piezoelectric scanners for SPMs are usually fabricated from lead zirconium titanate, or PZT, with various dopants added to create specific materials properties. Scanners are made by pressing together a powder, then sintering the material. The result is a polycrystalline solid. Each of the crystals in a piezoelectric material has its own electric dipole moment. These dipole moments are the basis of the scanner's ability to move in response to an applied voltage.

After sintering, the dipole moments within the scanner are randomly aligned. If the dipole moments are not aligned, the scanner has almost no ability to move. A process called poling is used to align the dipole moments. During poling the scanners are heated to about 200°C to free the dipoles, and a DC voltage is applied to the scanner. Within a matter of hours most of the dipoles become aligned. At that point, the scanner is cooled to freeze the dipoles into their aligned state. The newly poled scanner can then respond to voltages by extending and contracting.

Occasional use of the scanner will help maintain the scanner's polarization. The voltage applied to enact the scanning motion realigns the stray dipoles that relax into random orientation. If the scanner is not repoled by regular use, a significant fraction of the dipoles will begin to randomize (depolarize or depole) again over a period of weeks. Depoling is accelerated markedly if the scanner is subjected to temperatures above 150°C. This means that if you want to add a heated stage to your SPM, you must isolate it thermally from the scanner. (The Curie temperature for PZT materials is about 150°C.)

Many SPMs use variations of the simple tube design depicted in Figure 2-2. In this design, the scanner is a hollow tube.

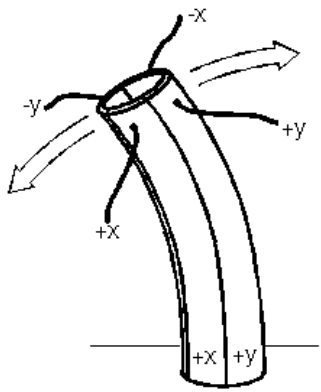

Figure 2-2. The scanner tube.

Electrodes are attached to the outside of the tube, segmenting it electrically into vertical quarters, for +x, +y, -x, and -y travel. An electrode is also attached to the center of the tube to provide motion in the z direction. When alternating voltages are applied to the +x and -x electrodes, for example, the induced strain of the tube causes it to bend back and forth in the x direction. Voltages applied to the z electrode cause the scanner to extend or contract vertically.

In most cases, the voltage applied to the z electrode of the scanner at each measurement point constitutes the AFM (constant-force) or the STM (constant-current) data set. In some cases, an external sensor is used to measure the height of the scanner directly (see §2.4). For the purposes of the discussion in the following sections, it is assumed that the data set consists of voltages applied to the z electrode.

The maximum scan size that can be achieved with a particular piezoelectric scanner depends upon the length of the scanner tube, the diameter of the tube, its wall thickness, and the strain coefficients of the particular piezoelectric ceramic from which it is fabricated. Typically, SPMs use scanners that can scan laterally from tens of angstroms to over 100 microns. In the vertical direction, SPM scanners can distinguish height variations from the sub-angstrom range to about 10 microns.

Piezoelectric scanners are critical elements in SPMs, valued for their sub-angstrom resolution, their compactness, and their high-speed response. However, along with these essential properties come some challenges.

2.2 Scanner Nonlinearities

As a first approximation, the strain in a piezoelectric scanner varies linearly with applied voltage. (Strain is the change in length divided by the original length, $\Delta l / l$.) The following equation describes the ideal relationship between the strain and an applied electric field:

$$s = d\,E$$

where s is the strain in Å/m, E is the electric field in V/m, and d is the strain coefficient in Å/V. The strain coefficient is characteristic of a given piezoelectric material.

In practice, the behavior of piezoelectric scanners is not so simple—the relationship between strain and electric field diverges from ideal linear behavior. These divergences are described in the following sections.

2.2.1 Intrinsic Nonlinearity

Suppose the applied voltages start from zero and gradually increase to some finite value. If the extension of the piezoelectric material is plotted as a function of the applied voltage, the plot is not a straight line, but an s-shaped curve, as seen in Figure 2-3. The dashed line in the graph is a linear fit to the data.

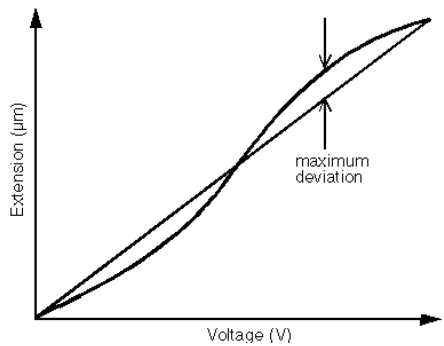

Figure 2-3. Intrinsic nonlinearity of a scanner.

The intrinsic nonlinearity of a piezoelectric material is the ratio of the maximum deviation Δy from the linear behavior to the ideal linear extension y at that voltage. In other words, the nonlinearity is $\Delta y/y$, expressed as a percentage. Intrinsic nonlinearity typically ranges from 2% to 25% in the piezoelectric materials used in SPM systems.

In the plane of the sample surface, the effect of intrinsic nonlinearity is distortion of the measurement grid of Figure 2-1. Because the scanner does not move linearly with applied voltage, the measurement points are not equally spaced. As a result, an SPM image of a surface with periodic structures will show non-uniform spacings and curvature of linear structures. Less regular surfaces may not show recognizable distortion, even though the distortion is present.

Perpendicular to the plane of the sample surface (in the z direction), intrinsic nonlinearity causes errors in height measurements. Height is usually calibrated for SPMs by scanning a sample with a known step height. By reading the voltage applied to the z electrode as it traverses the step, the z component of the strain coefficient can be calculated. However, if that strain coefficient is directly applied to measure a feature different in height from the calibrated height, the intrinsic nonlinearity of the scanner will generate errors.

2.2.2 Hysteresis

To complicate matters, piezoelectric ceramics display hysteretic behavior. Suppose we start at zero applied voltage, gradually increase the voltage to some finite value, and then decrease the voltage back to zero. If we plot the extension of the ceramic as a function of the applied voltage, the descending curve does not retrace the ascending curve—it follows a different path, as shown in Figure 2-4. Note that in this section it is assumed that the voltages change very slowly. Nonlinearities that result from time-dependent behavior of the piezoelectric ceramic are treated in the next section.

The hysteresis of a piezoelectric scanner is the ratio of the maximum divergence between the two curves to the maximum extension that a voltage can create in the scanner: $\Delta Y/Y_{max}$. Hysteresis can be as high as 20% in piezoelectric materials.

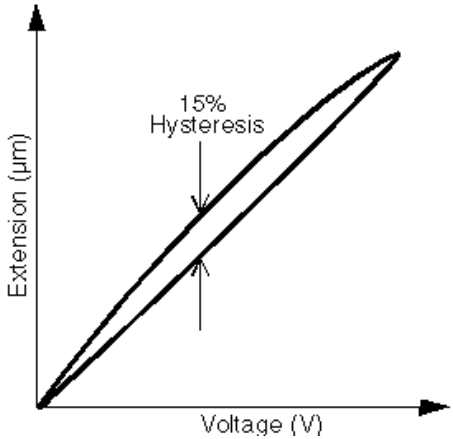

Figure 2-4. Hysteresis of a scanner.

As mentioned in the introduction to this chapter, SPM data are usually collected in one direction to minimize registration errors caused by scanner hysteresis. Figure 2-4 shows that data collected in the return direction would be shifted slightly, distorting the measurement grid of Figure 2-1. Since most SPMs today have provisions for taking scans in any fast-scan direction, you can observe hysteresis in the plane of the sample by comparing data sets taken in opposite fast-scan directions. For example, you could compare a data set taken left to right with a data set taken right to left. Scanner hysteresis would cause a shift between the data sets.

Hysteresis in the direction perpendicular to the plane of the sample causes erroneous step-height profiles, as shown in Figure 2-5. Referring to the curve of Figure 2-4, we see that if the scanner is going up a step in the z direction, a certain voltage is required to allow the scanner to contract. But going down the same step the scanner extends, and extension takes more voltage than contraction for the same displacement. When the SPM image is represented by the voltage applied to the scanner, a profile of the image would look like Figure 2-5. It is arbitrarily assumed in Figure 2-5 that the strain coefficient in z was calibrated for a contracting scanner.

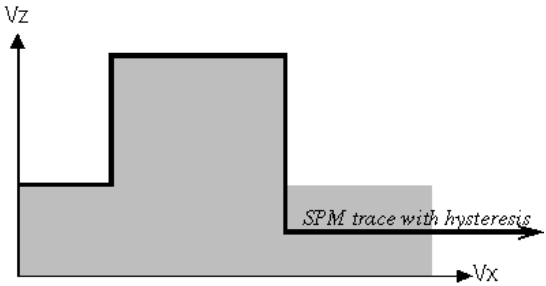

Figure 2-5. Effects of hysteresis on a step.

2.2.3 Creep

When an abrupt change in voltage is applied, the piezoelectric material does not change dimensions all at once. Instead, the dimensional change occurs in two steps: the first step takes place in less than a millisecond, the second on a much longer time scale. The second step, Δx_c in Figure 2-6, is known as creep.

Quantitatively, creep is the ratio of the second dimensional change to the first: $\Delta x_c/\Delta x$. Creep is expressed as a percentage and is usually quoted with the characteristic time interval T_{cr} over which the creep occurs. Typical values of creep range from 1% to 20%, over times ranging from 10 to 100 seconds.

The times involved during typical scans place the lateral motion of the scanner in the curved part of the response curve in Figure 2-6. As a result, two scans taken at different scan speeds show slightly different length scales (magnifications) when creep is present. You can trust only the measurement made at the scan speed that you used to calibrate your SPM when creep is present.

Another effect of creep in the plane of the sample is that it can slow down your work when you try to zoom in on a feature of interest. Suppose you want to characterize a defect on the surface of your sample. Most likely, you'll first take a large scan to find the defect. Suppose you see the defect, very tiny, in a corner of the large scan. What you would prefer to do is take a much smaller scan—a high-resolution scan—centered about the defect. An SPM applies an offset voltage to move the scanner to its new center position to take the second scan.

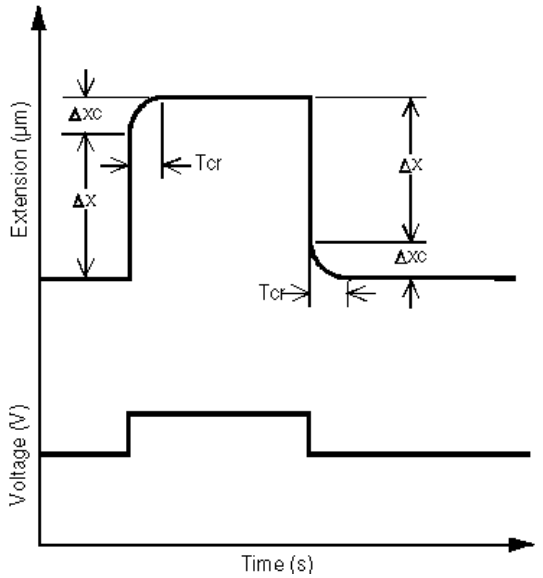

Figure 2-6. Plots showing creep of a scanner.

Because you have applied a sudden voltage step, in this case an offset voltage in the plane of the sample, creep will cause you to miss your target. If you continue to collect scans without changing the offset voltage, the scanner will continue to relax until the defect eventually drifts (creeps) into the center of your scan. The process will likely take a matter of minutes.

To examine the effects of creep in the z direction, consider a step as shown in Figure 2-7. As the tip traverses the step from bottom to top, the scanner contracts immediately with a voltage corresponding to the full step height. However, over the next few seconds the scanner continues to contract slowly as creep occurs. To keep the tip in contact with the sample, an SPM has to apply a voltage in the other direction, counteracting the creep. When the tip traverses the step from top to bottom, the same process occurs. The scanner extends to accommodate the step, then continues to creep. An SPM must apply a voltage in the opposite direction to maintain contact between the tip and the sample.

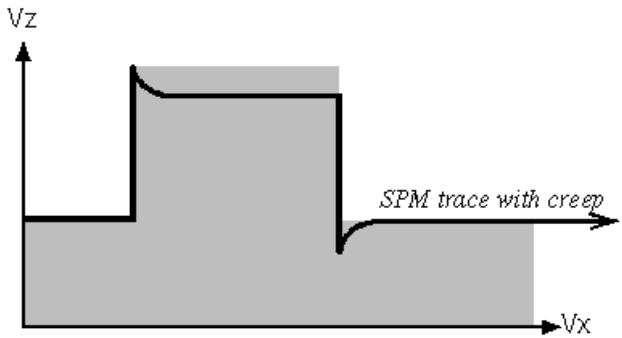

Figure 2-7. Effects of creep on a step.

The effect of creep on the profile of a step is a simple example. Consider a more typical sample with steep slopes that represent defects or grains or other surface features. Creep may cause an SPM image to look like it has ridges on one side of a feature and shadows on the other side of a feature. If there are shadows where the tip has just traveled down a steep slope, or ridges where the tip has just traveled up a steep slope, creep may be responsible. Reversing the fast-scan direction and taking the same image helps separate creep artifacts from true ridges and trenches (see §2.5.3).

2.2.4 Aging

The strain coefficient, d, of piezoelectric materials changes exponentially with time and use. Figure 2-8 graphs the aging of a piezoelectric scanner, for cases of both high and low voltage usage.

The aging rate is the change in strain coefficient per decade of time. When a scanner is not used, the deflection achieved for a given voltage gradually decreases. The aging rate of scanners for an SPM can produce a decrease in lateral strain coefficients (and therefore, an error in length measurements taken from SPM images) over time. When a scanner is used regularly, the deflection achieved for a given voltage increases slowly with use and time.

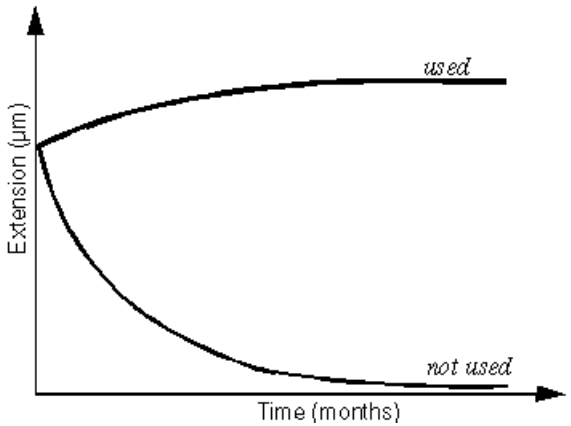

Figure 2-8. Aging of a scanner, with use or left idle.

These two phenomena are part of the same process. Recall from the introduction to this chapter that piezoelectric materials are polycrystalline ceramics. Each of the tiny crystals that compose the scanner has its own dipole moment. Repeated application of voltage in the same direction—such as the voltage applied during scanning—causes more and more of the dipoles to align themselves along the axis of the scanner. The amount of deflection achieved for a given voltage depends upon how many dipoles are aligned. Thus, the more the scanner is used, the farther the scanner will travel.

On the other hand, if the scanner is not used, the dipole moments of the crystals will gradually become randomly oriented again. As a result, fewer dipoles contribute to the deflection of the scanner. When you buy an SPM, the scanners have already been "poled," which means that they have already been exercised to the point where the deflection of the scanner is close to its maximum. The dependence of the scanner deflection on time and usage means that the scanner may not be extending the same distance for a given applied voltage as it did when it was first calibrated. As a result, when you measure a feature on an SPM image, the values of lateral and vertical dimensions may be in error.

2.2.5 Cross Coupling

The term cross coupling refers to the tendency of *x*-axis or *y*-axis scanner movement to have a spurious *z*-axis component (Figure 2-9). It arises from several sources and is fairly complex. For example, the electric field is not uniform across the scanner. The strain fields are not simple constants, but actually complex tensors. Some "cross talk" occurs between *x*, *y*, and *z* electrodes. But the largest effect is geometric. Geometric cross coupling has its basis in the way piezoelectric scanners are constructed, usually as segmented tubes or as tripods.

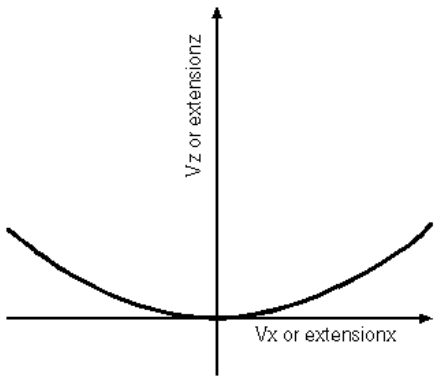

Figure 2-9. Cross coupling motion of the scanner.

The *x*-*y* motion of the scanner tube is produced when one side of the tube shrinks and the other side expands. As a result, a piezoelectric tube scans in an arc, not in a plane (see Figure 2-2). A voltage applied to move the piezoelectric tube along the x or y axis (parallel to the surface of the sample) necessitates that the scanner extend and contract along the z axis (perpendicular to the surface of the sample) to keep the tip in contact with the sample.

A tripod scanner is designed with three mutually perpendicular bars or tubes glued together at one end. This design is also susceptible to cross coupling because the three bars of piezoelectric material are attached to one another. When the x bar extends or contracts, it causes rotation of the y and z bars.

Cross coupling can cause an SPM to generate a bowl-shaped image of a flat sample. A profile of such an image is shown in Figure 2-10 with an example of a step.

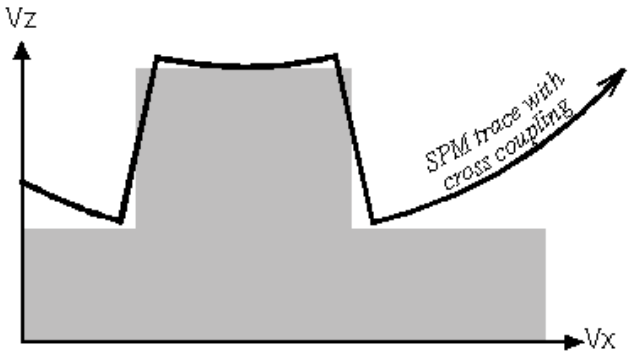

Figure 2-10. Effects of cross-coupling on a step.

In interpreting Figure 2-10, remember that the SPM image is based on the voltage required to compensate for the curvature generated by the arc of the scanner. The bowl shape may not always be evident in the final image because the curved background can be subtracted out using image-processing software. The best way to determine if the scanner is subject to cross coupling is to image a sample with a known radius of curvature, such as a lens. Software corrections can only flatten it or leave it alone. In the first case, you end up with a spuriously flat image, and in the second case the curvature of the scanner will be added to the curvature of the lens. The true curvature of a lens can be measured only when cross coupling is eliminated.

Throughout §2.2 the example of a single step to demonstrate hysteresis, creep, and cross coupling in the vertical direction is used. To show a single image in the laboratory that illustrates each of these effects in isolation is virtually impossible. Figure 2-11 shows the sum of the effects of hysteresis, creep, and cross coupling in the image of a single step. (The aspect ratio of the tip may also contribute to the shape of the sidewalls: see §3.3.)

Traditionally, the nonlinear behavior of piezoelectric scanners described above has been addressed imperfectly using software corrections. Some systems on the market use hardware solutions that eliminate most of the nonlinearities instead of correcting them. Hardware solutions are divided into optical, capacitive, and strain-gauge techniques. The best systems combine hardware and software corrections, using the strengths of each.

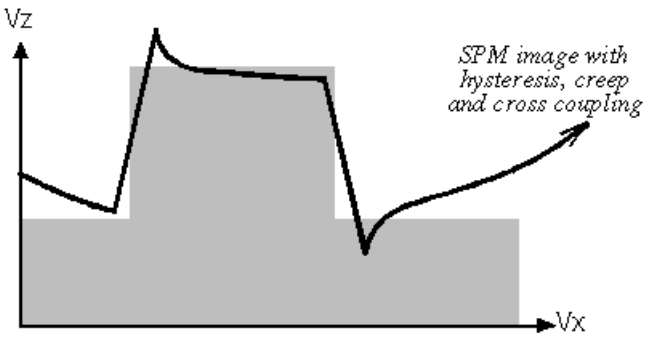

Figure 2-11. Effects of hysteresis, creep, and cross coupling on a step.

2.3 Software Correction

The first step in developing a software correction for scanner nonlinearities is to image a calibration grating. The system compares the measured data with the known characteristics of the grating. Then the system determines how to adjust the measured data to conform to the known characteristics. It stores that information in a file, or lookup table. Afterwards, the system can compensate for nonlinearity while collecting data by adjusting the voltage applied to the scanner in accordance with the file or the look-up table, as shown in Figure 2-12.

More sophisticated software correction algorithms include equations that model the scanner tube's non-linear response to applied voltages. The equations are used to calculate the voltages that are applied to the scanner to position it during a scan. Again, scanner calibration procedures are necessary to determine parameters for the algorithm.

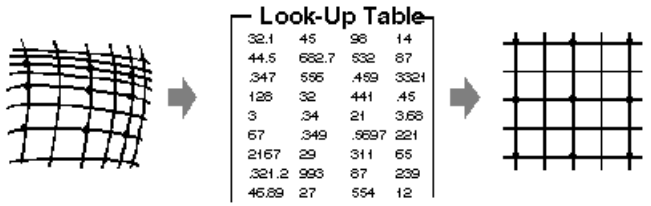

Figure 2-12. Software correction, shown using a look-up table.

Software solutions in general are relatively simple and inexpensive to implement. Their main disadvantage is that they compensate only partially for scanner nonlinearities. The corrections are strongly dependent upon the scan speed, scan direction, and whether the scanner was centered within its scan range during calibration. As a result, software corrections are most accurate only for scans that reproduce the conditions under which the calibration was done.

A scanner should be re-calibrated when scan conditions change. In practice, SPM systems that use only software corrections may vary from true linear behavior by as much as 10%. Often this deviation is unnoticed by the SPM user who calibrates and checks the calibration of the SPM with the same procedure every time.

2.4 Hardware Correction

Systems with hardware solutions sense the scanner's actual position with external sensors, as illustrated in Figure 2-13. The signal read from the sensor of each axis is compared to a signal that represents the intended scanner position along that axis. A feedback system applies voltage to the scanner to drive it to the desired position. In this way, the scanner can be driven in a linear fashion. The external sensors themselves must be stable and immune to all sources of nonlinearity, since their purpose is to improve the linearity of the SPM.

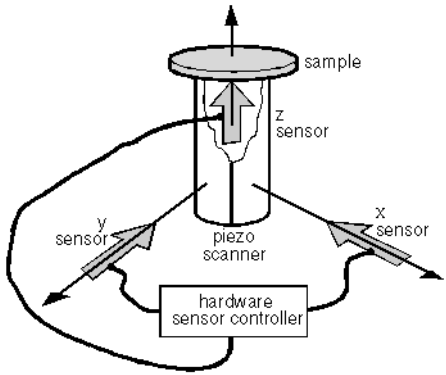

Figure 2-13. Schematic of a scanner, showing external detectors.

Because the scanner's actual position is measured, systems using hardware sensors compensate for intrinsic nonlinearity, hysteresis, creep, aging, and cross coupling. They can reduce the total nonlinearity of the system to less than 1%.

Figure 2-14 illustrates how SPMs equipped with hardware correction enable you to zoom in on a feature of interest in an image without the effects of creep. The left image is a 40µm scan of a grating. The box in the image shows the intended location of the zoomed scan. The right image is the zoomed 2µm scan of that location. An image of the same area acquired at a later time would look identical to the right image, indicating that creep is not present in SPMs with hardware correction schemes.

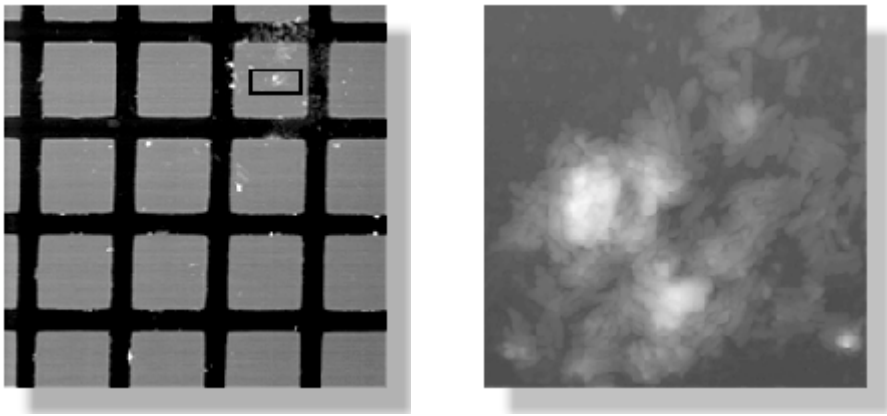

Figure 2-14. Images of a grating, demonstrating the ability of systems with hardware correction to zoom in on a feature of interest.

2.4.1 Optical Techniques

In optical solutions to scanner nonlinearity, a "flag," or reflector, is attached to the scanner. A light shines on the flag, and a detector responding to either the phase or the position of the light determines the actual position of the scanner. The system then uses feedback to adjust the voltage to the scanner to place it in the proper position to generate a linear scan.

2.4.2 Capacitive Techniques

In capacitive solutions, a metal electrode is placed on the scanner and another is mounted nearby. An electrical circuit then measures the capacitance between the electrodes, which varies with their separation. Having located the scanner in this way, the system uses feedback to adjust the scanner's position to compensate for nonlinearity.

2.4.3 Strain-gauge Techniques

In strain-gauge solutions to scanner nonlinearities, a strain gauge is mounted on the scanner. The active element in a strain gauge is a piece of piezoresistive material—material whose resistance varies when it is under tensile or

compressive stress. When the scanner moves, the resistance in the strain gauge changes. The magnitude of the resistance of the strain gauge reflects the amount of bending in the scanner, thereby measuring its position. An SPM uses feedback to adjust the scanner's position and to generate a linear scan.

2.5 Tests for Scanner Linearity

If you suspect that nonlinear behavior of the piezoelectric scanner has created artifacts in an SPM image, you can perform various tests. This section describes the symptoms and gives a test procedure to identify each source of nonlinearity. When you are evaluating an SPM, make sure that it has adequate compensation for intrinsic nonlinearity, hysteresis, creep, aging, and cross coupling. Otherwise, your SPM images may be distorted, the measurements you make from them may be erroneous, and the conclusions you draw from your measurements may lead you astray.

2.5.1 Intrinsic Nonlinearity

X-Y Plane

Symptom: Non-uniform spacings and curvature appear in structures that you know or believe to be linear, as shown in Figure 2-15.

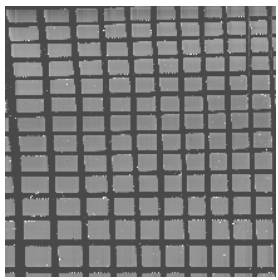

Figure 2-15. Image of a grating, showing non-uniform spacing and curvature.

Test: Image a calibration grating. The image should show consistent spacing and straight lines.

Z Axis

Symptom: Instrument measures heights inaccurately.

Test: Measure a wide range of heights using known height standards.

2.5.2 Hysteresis

X-Y Plane

Symptom: Displacement is observed in comparing images of the same structure taken using different fast-scan directions.

Test: Image the same surface with left-to-right fast-scan direction, then with right-to-left fast-scan direction. Or, compare a top-to-bottom scan with a bottom-to-top scan. The images should be identical.

Z Axis

Symptom: Slopes of sidewalls of features depends upon whether the scanner is moving up or down the slope. See Figure 2-18 at the end of this chapter, which shows hysteresis, creep, and cross coupling.

Test: Measure a step and compare the slopes of the edge profiles.

2.5.3 Creep

X-Y Plane: For SPMs Equipped with Software Correction

Symptom: Right after you move to a new area to start a new scan (by offsetting the scanner, not by translating a stage), the features in the image drift around for a few minutes before settling (see Figure 2-16).

Test: Take a large scan with a recognizable feature in one corner. Take a second scan, ten times smaller (ten times higher magnification) centered on that feature. In the presence of creep, the system will not center properly on the feature the first time you scan. Repeated scans should bring the feature to the center of the scan, as the scanner relaxes to its equilibrium position. This relaxation is demonstrated nicely in the series shown in Figure 2-16, with scans taken approximately one minute apart. Each scan took just less than one minute to complete.

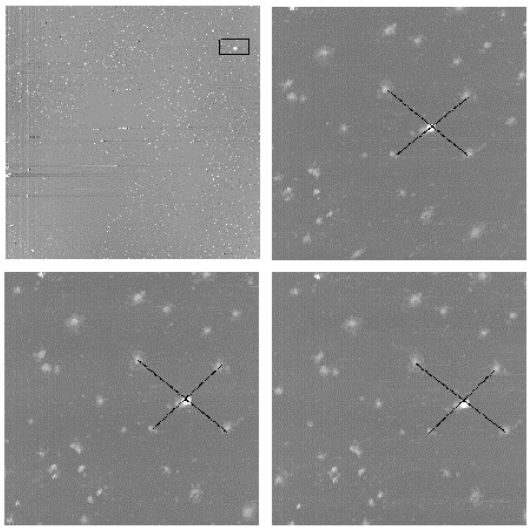

Figure 2-16. Images showing the effects of creep.

In Figure 2-16, the top left image is a large scan of a silicon surface with defects. The box in the image shows the location intended for the zoomed scan. When creep is eliminated, zooming in on this location is fast and precise. The top right image shows the zoomed location, and was acquired about 1 minute after the top left image was acquired. The position of five defects in the image is marked for reference. Note the diagonal streaking in the lower part of the image, indicating

that scanner creep was considerable during the scan. The bottom left image was acquired about 2 minutes after the top left image was acquired. No streaking is present in the image, indicating that creep has slowed. Reference defects are still settling into their final positions. The bottom right image was acquired about 3 minutes after the top left image. Reference defects have moved less during the third minute, as creep comes to an end and the scanner attains its relaxed position.

It is important to note that the images in Figure 2-16 were acquired with a system that uses software correction schemes. Scanner creep as depicted in Figure 2-16 is eliminated when an SPM equipped with hardware correction is used to acquire data. In this case, the three images of the zoomed-in feature taken 1 minute apart would be identical. (See §2.4.)

Z Axis

Symptom: Profiles of the top and the bottom of a step show exponential decay, forming ridges and trenches as the scanner creeps in response to the sudden changes in voltage necessary to allow the tip to negotiate the step. (See the graph showing hysteresis, creep, and cross coupling, Figure 2-18.)

Test: Evaluate the image of a rectangular step with known characteristics.

2.5.4 Aging

X-Y Plane

Symptom: Lateral calibration of the SPM changes over time.

Test: Test the stability over time of measurements of known lateral spacings using a calibration grating.

Z Axis

Symptom: Height calibration of the SPM changes over time.

Test: Test the stability over time of height measurements using known height standards.

2.5.5 Cross Coupling

Symptom: SPM image shows a curved surface on a sample that you know or believe to be flat, as depicted in Figure 2-17. Or, you see erroneous curvature on a sample with known curvature. Note the bright and dark diagonal corners in the image shown in Figure 2-17. These corners show imperfect software flattening. In the absence of cross coupling, the image would be as flat as the true surface.

Test: Image a surface that you know is flat, or a surface with known curvature.

Figure 2-17. Image of a flat sample, with scanner curvature removed using image-processing software.

2.5.6 Step Profile: Hysteresis, Creep, and Cross Coupling in Z

The cumulative effects of scanner hysteresis, creep, and cross coupling are demonstrated in Figure 2-18.

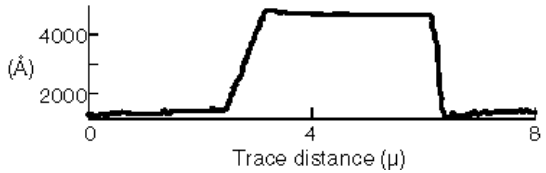

Figure 2-18. Profile of a step, showing hysteresis, creep, and cross coupling.

Scanner hysteresis causes the upward and downward sidewalls of the step to have different slopes, because the voltage required to contract the scanner as the tip goes up the step is smaller than the voltage required to extend the scanner as the tip goes down the step. Creep causes the exponential decay that makes the left side of the top of the step higher than the right side. And cross coupling adds curvature to the entire profile.

2.6 Further Reading

The Piezo Book, Burleigh Instruments, Product information on the fundamentals of piezo materials.

P. Atherton, "Micropositioning Using Piezoelectric Translators," Photonics Spectra, Dec. 1987, pp. 51-45.

J.E. Griffith, G.L. Miller, and C.A. Green, "A Scanning Tunneling Microscope with a Capacitance-based Position Monitor," J. Vac. Sci. Technol. B, vol. 8, No. 6, Nov/Dec 1990, pp. 2023-2027.

R.C. Barrett and C.F. Quate, "Optical Scan-correction System Applied to Atomic Force Microscopy," Rev. Sci. Instrum. 62(6), 1393 (1991).

CHAPTER 3
SPM PROBES

3.1 Introduction

The probe is a critical component of a scanning probe microscope because different probes can measure different properties of the sample. Also the probe determines the force applied to the sample and the ultimate resolution of the system.

The most common probes in scanning probe microscopy are the cantilevers. These cantilevered probes are highly suited to measure the topography of a sample. Using different coating on the cantilevers different properties of the sample can be measured, like magnetic (MFM), electrostatic (EFM), capacitance (SCM) etc. Other types of probes are available to measure other properties, like optical (NSOM), thermal (SThM), electronic (STM).

3.2 Cantilevers

Figure 3-1 depicts a scanning electron microscopy (SEM) image of a cantilever.

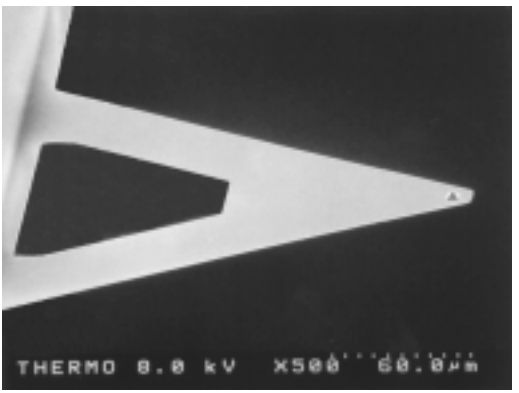

Figure 3-1. SEM image of a cantilever (Microlever™, cantilever A).

Integrated tip and cantilever assemblies can be fabricated from silicon or silicon nitride using photolithographic techniques. More than 1,000 tip and cantilever assemblies can be produced on a single silicon wafer. V-shaped cantilevers are the most popular, providing low mechanical resistance to vertical deflection, and high resistance to lateral torsion. Cantilevers typically range from 100 to 200μm in length, 10 to 40μm in width, and 0.3 to 2μm in thickness (see Figure 3-2).

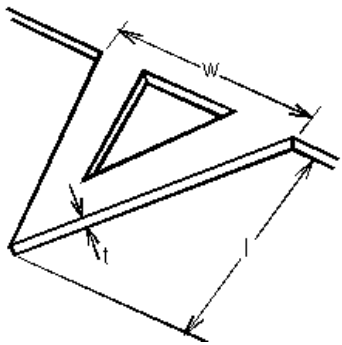

Figure 3-2. V-shaped cantilever, showing length (l), width (w), and thickness (t).

3.2.1 Properties of Cantilevers

Atomic force microscopes require not only sharp tips, but also cantilevers with optimized spring constants—lower than the spring constants between atoms in a solid, which are on the order of 10N/m. The spring constant of the cantilever depends on its shape, its dimensions, and the material from which it is fabricated. Thicker and shorter cantilevers tend to be stiffer and have higher resonant frequencies. The spring constants of commercially available cantilevers range over four orders of magnitude, from thousandths of a Newton per meter to tens of Newton's per meter. Resonant frequencies range from a few kilohertz to hundreds of kilohertz providing high-speed response and allowing for non-contact AFM operation.

3.3 Tip Shape and Resolution

The lateral resolution of an AFM image is determined by two factors: the step size of the image (see Figure 2-1), and the minimum radius of the tip. Consider an image taken with 512 by 512 data points. Such a scan 1µm by 1µm would have a step size—and lateral resolution—of (1µm ÷ 512 =) about 20Å.

The sharpest tips available commercially can have a radius as small as 50Å. Because the interaction area between the tip and the sample is a fraction of the tip radius, these tips typically provide a lateral resolution of 10 to 20Å. Thus, the resolution of AFM images larger than 1µm by 1µm is usually determined not by the tip but by the image's step size. The quoted *best resolution* of an AFM, however, depends upon how resolution is defined.

In the microscopy community, two asperities (peaks) are considered resolved if the image satisfies Rayleigh's criterion. In this application, Rayleigh's criterion requires that the height of the image dip at least 19% between the asperities, as illustrated in Figure 3-3.

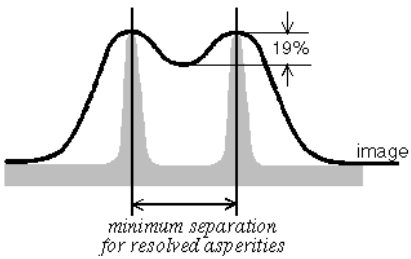

Figure 3-3. Definition of lateral resolution using Rayleigh's criterion.

To determine the lateral resolution of an SPM experimentally, the asperities are brought closer and closer together until the image no longer dips by 19% between peaks. The minimum separation between resolved asperities determines the best lateral resolution of the system. Using this definition, the lateral resolution of an AFM with the sharpest tips commercially available is 10 to 20Å.

At first glance the figure of 10 to 20Å resolution seems to conflict with the ubiquitous images of atomic lattices in AFM brochures. The distinction between

imaging atomic-scale features with accurate lattice spacing and symmetry, and *true atomic resolution* bears some comment.

An STM gives true atomic resolution. Because the dependence of the tunneling current on the tip-to-sample separation is exponential, only the closest atom on a good STM tip interacts with the closest atom on the sample, as shown in Figure 3-4, top. For AFMs, the dependence of cantilever deflection on tip-to-sample separation is weaker. The result is that several atoms on the tip interact simultaneously with several atoms on the sample, shown in Figure 3-4, bottom.

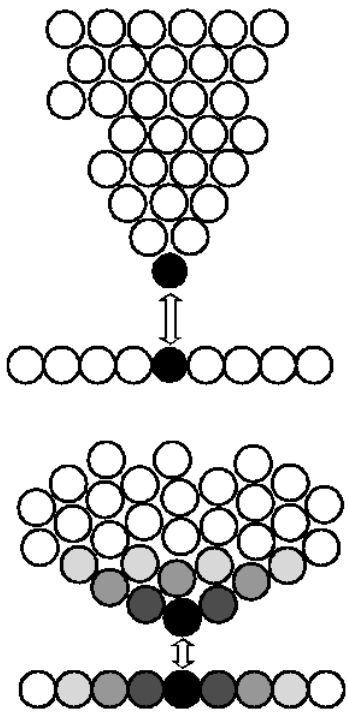

Figure 3-4. Interatomic interaction for STM (top) and AFM (bottom). Shading shows interaction strength.

For AFMs, each atom of the tip that participates in imaging (each shaded atom in Figure 3-4, bottom) "sees" the sample as a periodic lattice. But because the

atoms of the tip are in different lateral positions, the lattice that each atom sees is shifted from the lattice seen by its neighbors, as shown in Figure 3-5.

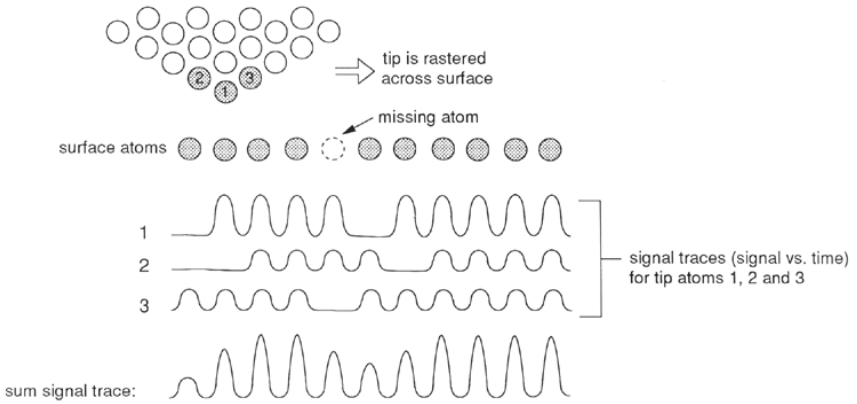

Figure 3-5. AFM scan of atomic-scale periodic lattice, showing the sum of the contributions from each atom at each instant in time.

Each atom in the tip is also at a different height with respect to the sample. The strength of the signal seen by each tip atom weakens with its distance from the sample. When the contributions from all of the participating atoms in the tip are combined at each snapshot in time, and the result is summed over time as the tip is scanned across the periodic surface, the final image is periodic with the correct symmetry and spacings. However, if one atom were missing, the hole left behind would not be detected because the image represents a superposition of many images. (See Figure 3-5.) For true atomic resolution, a single missing atom must be detectable. Thus, generating an atomic-scale image of a periodic lattice—which is possible using contact AFM—does not imply that true atomic resolution has been achieved.

For both contact and non-contact imaging, you should choose a tip that is sharper than the smallest features on your sample. If the tip is larger than the surface features, an artifact know as *tip imaging* occurs. Tip imaging is discussed in detail in §4.1. You may not always want to choose the sharpest tip available, since the sharpest tips are more expensive and can be less durable. You need the sharpest tips only when you require the best resolution.

For LFM, blunter tips can be preferable precisely because they present a larger interaction area between tip and sample. A larger area of interaction can produce a stronger lateral deflection of the cantilever. The larger cantilever deflection must be balanced against the lower lateral resolution delivered by the blunter tip.

AFM manufacturers offer microfabricated tips in three geometries: pyramidal, tetrahedral, and conical. Conical tips can be made sharp, with high aspect ratios (the ratio of tip length to tip width). Tip radii as small as 50Å have been observed. Pyramidal tips have lower aspect ratios and nominal tip radii of a few hundred angstroms, but they are more durable.

AFM tips are fabricated from silicon or silicon nitride. The fabrication process is different for the two materials. The features of tips made from each material are governed by the fabrication process as well as the material properties.

Silicon conical tips are made by etching into the silicon around a silicon dioxide cap. The high aspect ratio of conical tips makes them suitable for imaging deep, narrow features such as trenches, but they may break more easily than the

pyramidal or tetrahedral geometries, as described above. Silicon also has the advantage that it can be doped, so that tips can be made electrically conducting. Conducting tips are useful for controlling the bias between the tip and the sample, or for preventing unwanted charge buildup on the tip.

Silicon nitride tips are fabricated by depositing a layer of silicon nitride over an etched pit in a crystalline silicon surface, as illustrated in Figure 3-6. This method produces the pyramidal or tetrahedral tip geometry. The aspect ratio of a silicon nitride tip is thus limited by the crystallographic structure of the etch pit material, silicon. The tips are broader than conical silicon tips, making them sturdier but less suitable for imaging deep, narrow features. Silicon nitride is a harder material than silicon, which also makes silicon nitride tips more durable than silicon tips.

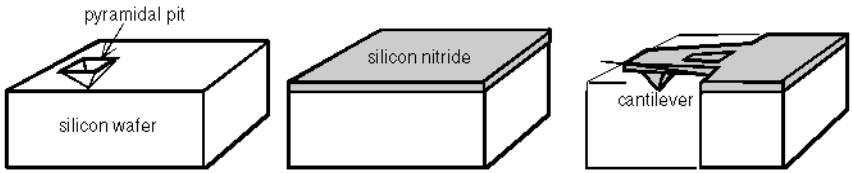

Figure 3-6. Fabricating a silicon nitride tip.

Silicon nitride films, however, contain residual stresses which make them deform as the film thickness increases. For this reason, applications that call for thick cantilevers—or cantilevers with high resonant frequencies—use silicon cantilevers. The thickness of silicon nitride cantilevers is usually less than one micron, whereas silicon cantilevers can be several microns thick.

A more specialized type of cantilever that has a tip grown in a scanning electron microscope is also available commercially. (A specialized tip can also be produced by "milling" an existing tip using a focused ion beam.) The SEM is used in an unusual way: to deposit contamination in a column. The tips are not microfabricated in bulk; they are grown one at a time on top of a bare cantilever or square-pyramidal tip. These tips have the advantage of almost unlimited aspect ratio. However, they are not normally sharp, and can bend or break easily.

3.4 How to Select a Probe

The desirable properties for a probe depend on the imaging mode and the application. In contact mode, soft cantilevers are preferable because they deflect without deforming the surface of the sample, a silicon nitride Microlever™ would be a good choice for most applications.

In non-contact mode, stiff cantilevers with high resonant frequencies give optimal results. Here the non-contact silicon Ultralevers™ are suited for most non-contact applications. Also on non-conductive samples which silicon tips may be preferred to prevent unwanted charge build-up in the tip.

For other applications than topography, like MFM, NSOM, SThM (thermal) etc., different types of probes have to be used. Table 3-1 gives an overview of probe types used for these special applications.

Table 3-2 gives a general selection tree that may help you to select a probe. Please keep in mind that the choices made may not be optimized for your specific application, and therefore a different probe could be more suited than listed here. Table 3-3 lists the different model numbers available for a recommended probe type. The probes are available mounted on AutoProbe mounts, mounted on TopoMetrix mounts or unmounted in pre-separated quantities or as a half wafer. More details for the different model numbers can be found through the ThermoMicroscopes SPM Probe web site at http:\\www.spmprobes.com.

Table 3-1: Probe selection for special applications

Probe Selection Criteria		Probe Model Numbers		
Application Type	*Recommended Probe Type*	Mounted for AutoProbe™ Instruments	Mounted for TopoMetrix™ Instruments	Unmounted and for all other SPMs
EFM	*tips coated with a conductive material*	ULNC-MFMT-AB (qty 25) ULNC-MFMT-CD (qty 25) MSNC-MFMT-A (qty 25) MSNC-MFMT-B (qty 25)[1]	1600-00 (qty 8)	ULNC-MFNM (qty 25) MSNC-MFNM (qty 25)
MFM	*tips coated with a magnetic material*	ULNC-MFMT-AB (qty 25) ULNC-MFMT-CD (qty 25) MSNC-MFMT-A (qty 25) MSNC-MFMT-B (qty 25)	1670-00 (qty(8)	ULNC-MFNM (qty 25) MSNC-MFNM (qty 25)
NSOM	*optical fiber NSOM probe, with or without Accutune™ tuning fork system*		1640-00 (qty10) 1642-00 (qty 5) 1720-00 (qty 10)	
Thermal	*thermal probe*	CLST-NOMB (qty 5)	1610-00 (qty 10) 1615-00 (qty 5)	
STM	*tungsten or Pt/Ir wire, cut or etched*		2520-00 (qty 20) 2540-00 (qty 20) 2560-00 (qty 20)	2520-00 (qty 20) 2540-00 (qty 20) 2560-00 (qty 20)
SCM	*tips coated with a conductive material and with connector*	ULNC-SCMT-M5 (qty25) ULNC-SCMT-NKN (qty 25)		
Vacuum	*self sensing cantilevers, model Piezolever™*	PLCT-VPMT (qty 5 PLNC-VPMT (qty 5)		
Force Calibration	*model Force Calibration Cantilevers*	CLFC-NOMB (qty 5)		CLFC-NOBO (qty 5)
Piezolevers for AutoProbe SA	*self sensing cantilevers, model Piezolever™*	PLCT-SAMT (qty 5) PLNC-SAMT (qty 5)		

[1] Because of their high doping concentration regular Ultralevers may be used too.

Table 3-2: Probe Selection Tree

Probe Selection Criteria								
Application Type	sample type	sample static	sample side wall angles	tip durability	resolution	*recommended probe type*	reflection coated	Recommended Probe Category
Topography	hard (contact)	not static **A**	<45º	standard	standard	*silicon nitride cantilevers for contact mode, model Microlever™*	yes	❶
							no	❷
					highest	*sharpened silicon nitride cantilevers for contact mode, model Sharpened Microlever*	yes	❸
							no	❹
			45º-75º	standard	highest	*silicon conical tips for contact mode, model Ultralever™*	yes	❺
				extra		*diamond coated silicon tips for contact mode, model Ultralever*	yes	❻
			>75º	standard	highest	*silicon nitride tip with e-beam deposited needle for contact mode, model SuperTips™*	yes	❼
		is static ⇒ use non-contact mode (→**B**) and/or use an ionizer (→**A**)						
	soft **B** (non-contact)		<75º	standard	highest	*silicon cantilevers for non-contact mode, model Ultralever or dLever™*	yes	❽
				extra		*diamond coated silicon tips for non-contact mode, model Ultralever*	yes	❾
			>75º **C**	standard	highest	*high aspect ratio FIB tips, for non-contact model*	yes	❿

Table 3-3: Recommended Probe Models

Probe Model Numbers			
Recommended Probe Category	Mounted for AutoProbe™ Instruments	Mounted for TopoMetrix™ Instruments	Unmounted and for all other SPMs
❶	MLCT-AUMT-A (qty 25) MLCT-AUMT-BF (qty 25)	1520-00 (qty 20) 1525-00 (qty 10) 1530-00 (qty 20) 1870-00 (qty 20) (for Observer™)	MLCT-AUHW (half wafer) MLCT-AUNM (qty 25) 1590-00 (wafer)
❷	MLCT-NOMT-A (qty 25) MLCT-NOMT-BF (qty 25)		MLCT-NOHW (half wafer) MLCT-NONM (qty 25)
❸	MSCT-AUMT-A (qty 25) MSCT-AUMT-BF (qty 25)		MSCT-AUHW (half wafer) MSCT-AUNM (qty 25)
❹	MSCT-NOMT-A (qty 25) MSCT-NOMT-BF (qty 25)		MSCT-NOHW (half wafer) MSCT-NONM (qty 25)
❺	ULCT-AUMT-AB (qty 25) ULCT-AUMT-CD (qty 25)	1950-00 (qty 8)	ULCT-AUHW (half wafer) ULCT-AUNM (qty 25)
❻	ULCT-DCMB-AB (qty 25) ULCT-DCMB-CD (qty 25)		ULCT-DCBO (qty 5)
❼	see Table 3-2 **C**	1700-00 (qty 10) find more at Table 3-2 **C**	
❽	ULNC-AUMT-AB (qty 25) ULNC-AUMT-CD (qty 25) 1920-00 (qty 25)	1910-00 (qty 10) 1650-00 (qty 8) 1660-00 (qty 8)	ULNC-AUHW (half wafer) ULNC-AUNM (qty 25) 1900-00 (half wafer) 1930-00 (qty 25)
❾	ULNC-DCMB-AB (qty 5) ULNC-DCMB-CD (qty 5)	1894-00 (qty 4)	ULNC-DCBO (qty 5)
❿	ULNC-FBMB (qty 5)	1895-00 (qty 4)	ULNC-FBBO (qty 5)

Detailed information on the different probe models can be found through the ThermoMicroscopes SPM Probes web site at http://www.spmprobes.com. The site lists all specifications of the different probes, which are also available for download in PDF format for convenience. Through the web site probes can be ordered on-line using a credit card or the site can be used to compile a requisition for purchase orders.

For applications other than topography the probes are listed in Table 3-1.

3.5 Probe Handling

Under normal operating conditions, an AFM tip should last for a couple of days, so changing the probe should be a straightforward process. However, the chips upon which cantilevers are mounted are very small and can be unwieldy to handle. New designs permit pre-aligned, pre-mounted probes to be changed very quickly, with minimal alignment of the beam-bounce detection system. As with the user interface, you should evaluate how difficult it is to change a probe. Change a probe yourself, instead of watching a highly skilled operator change it.

3.6 Further Reading

H.A. Mizes, Sang-il Park, and W.A. Harrison, "Multiple-tip Interpretation of Anomalous Scanning-tunneling-microscopy Images of Layered Materials," Physical Review B, vol. 36, No. 8, pp. 4491-4494.

S. Akamine, T.R. Albrecht, M.J. Zdeblick, and C.F. Quate, IEEE Electr. Dev. Lett., 10, 489, 1989.

J.E. Griffith, D.A. Grigg, M.J. Vasile, P.E. Russell and E.A. Fitzgerald, "Characterization of Scanning Probe Tips for Linewidth Measurement," J. Vac. Sci. Technol. B 9 (6), Nov/Dec 1991.

J.E. Griffith, D.A. Grigg, M.J. Vasile, P.E. Russell, E.A. Fitzgerald, "Characterization of Scanning Probe Microscope Tips for Linewidth Measurement," J. Vac. Sci. Technol. B 9 (6), Nov/Dec 1991, pp. 3586-3589.

M. Radmacher, R.W. Tillmann, M. Fritz, H.E. Gaub, "From Molecules to Cells: Imaging Soft Samples with the Atomic Force Microscope," Science, vol. 257, Sept. 25, 1992, pp. 1900-1905.

F.J. Giessibl, Phys. Rev. B, 45 (23), 13815 (1992).

F.J. Giessibl, "Theory for an Electrostatic Imaging Mechanism Allowing Atomic Resolution of Ionic Crystals by Atomic Force Microscopy," Physical Review B, vol. 45, No. 23, 1992, pp. 13815-13818.

Jeffrey L. Hutter and John Bechhoefer, "Calibration of Atomic Force Microscope Tips," Reviews of Scientific Instruments, vol. 64, 1993, pp. 1868-1873.

C.W. Yuan, E. Batalla, A. de Lozanne, M. Kirk, and M. Tortonese, "Low Temperature Magnetic Force Microscope Utilizing a Piezoresistive Cantilever," Appl. Phys. Lett. 65, 1994, pp. 1308-1310.

U. Stahl, C.W. Yuan, A.L. de Lozanne, and M. Tortonese, "Atomic Force Microscope Using Piezoresistive Cantilevers and Combined with a Scanning Electron Microscope," Appl. Phys. Lett. 65, 1994, pp. 2878-2880.

CHAPTER 4
IMAGE ARTIFACTS

SPM images are among the easiest to interpret of images generated by any microscopy technique. With an electron or optical microscope, contrast is based on complex electromagnetic diffraction effects. Determining whether a feature is protruding from the surface or recessed into it can be difficult with an image from an optical or electron microscope. SPMs, however, collect three-dimensional data. In an SPM image, a peak is unambiguously a peak, and a valley is clearly a valley. With an optical or electron microscope, artificial contrast can occur when a sample consists of reflecting material embedded in an absorbing matrix, for example. SPMs, on the other hand, are largely indifferent to variations in optical or electronic properties, and measure true surface topography.

Despite the apparent simplicity of images from SPMs, SPM images are subject to some artifacts of their own. Fortunately, artifacts are relatively easy to identify. This section addresses the most common artifacts encountered in SPM imaging.

4.1 Tip Convolution

Most imaging artifacts in an SPM image arise from a phenomenon known as tip convolution or tip imaging. Every data point in an image represents a spatial convolution (in the general sense, not in the sense of Fourier analysis) of the shape of the tip and the shape of the feature imaged. As long as the tip is much sharper than the feature, the true edge profile of the feature is represented. However, when the feature is sharper than the tip, the image will be dominated by the shape of the tip. Figure 4-1 demonstrates the origin of tip convolution.

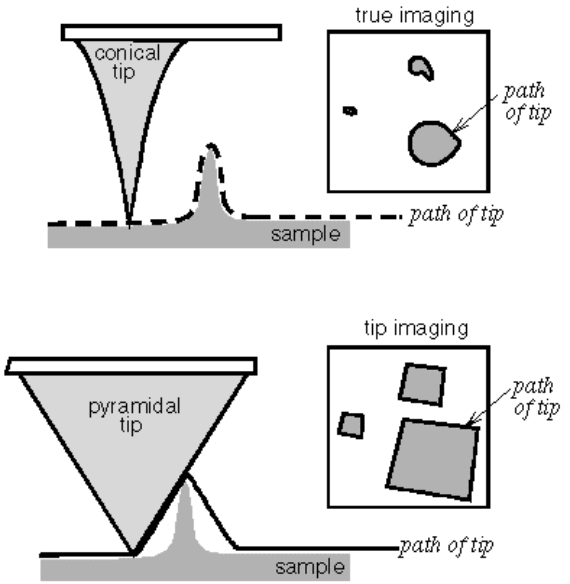

Figure 4-1. Comparison between true imaging and tip imaging.

The first commercial AFM tips were square pyramidal, formed by CVD deposition of Si_3N_4 on an etch pit in Si (100). The etch pit is bounded by (111) faces, which means that the resulting tip has a sidewall angle of about 62.5° along the flat side of the pyramid (45° along the corner edge of the pyramid). If such a tip is used, the edge profiles of SPM images of all features with sides steeper than 62.5° are dominated by the profile of the tip. Tips with higher aspect ratios have been marketed successfully since then, but microfabricated tips remain limited to a sidewall angle of about 80°. Further enhancement of the sidewall angle of the tip can result in degraded durability, or even bending of the tip during scanning.

Because many samples have features with steep sides, tip imaging is a common occurrence in images. Sidewall angles on images should be measured routinely, to determine whether the slope is limited by that of the tip, or truly represents the topography of the sample. One consolation is that the height of the feature is

reproduced accurately as long as the tip touches bottom between features. Thus, height measurements remain fairly accurate. The lateral dimensions from a tip-imaged scan, on the other hand, can provide the user with only a maximum value. In other words, if you measure a tip-imaged feature as having a width of 200Å, you'll know that the feature is at most 200Å wide.

To recognize tip imaging, look for a particular shape that is repeated throughout an image. The shape can be different sizes as the tip is convolved with features of different sizes, but it will always maintain the same orientation. If you suspect tip imaging is occurring, you can rotate your sample and image it again. If the tip is dominating the image, the orientation of the tip shape will be the same before and after rotation. If the image is a true representation of the surface, the shapes in the image will rotate along with the sample. This test is represented schematically in Figure 4-2. If your image is dominated by tip-convolution effects, change to another tip.

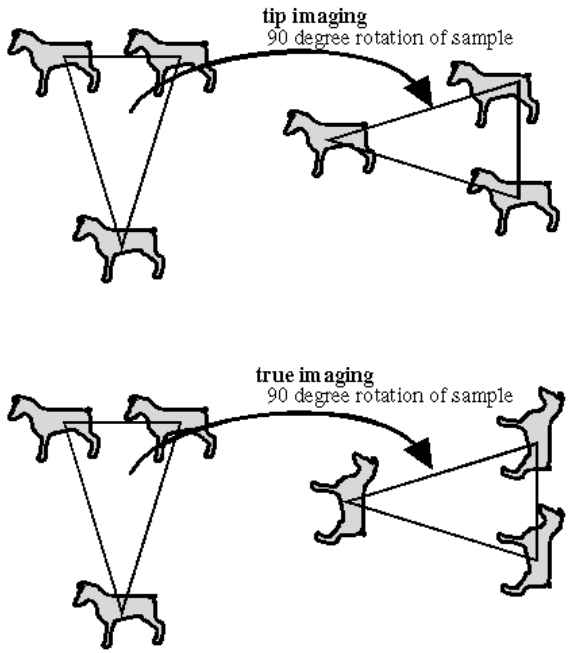

Figure 4-2. Top-down image showing characteristically shaped features.

For STM, the imaging portion of the tip is formed by an atom or cluster of atoms at the end of a long wire. Because the dependence of the tunneling current upon the tip-to-sample distance is exponential, the closest atom on the tip will image the closest atom on the sample.

If two atoms on the tip are equidistant from the surface, all of the features in the image will appear doubled. This is an example of multiple-tip imaging. The best way to alleviate this problem is to apply a voltage pulse to change the tip configuration by field emission. Alternatively, you can press the tip gently against the sample to form a new tip shape, and take another image.

4.2 Convolution with Other Physics

Another common category of SPM artifacts derives from the sensitivity of an SPM to physical properties other than those responsible for mapping the surface topography. For example, regions of variable conductivity are convolved with topographic features for STM, and soft or elastic surfaces can deform under the pressure of the AFM tip.

4.3 Feedback Artifacts

If the feedback loop of an SPM is not optimized, the SPM image can be affected. When feedback gains are too high the system can oscillate, generating high frequency periodic noise in the image. This may occur throughout the image or be localized to features with steep slopes.

On the other hand, when feedback gains are too low, the tip cannot track the surface well. In the extreme case, the image loses detail, appearing smooth or "fuzzy." A less obvious effect is "ghosting." On sharp slopes, an overshoot can appear in the image as the tip travels up the slope, and an undershoot can appear as the tip travels down the slope. This feedback artifact commonly appears on steep features, represented as bright ridges on the uphill side and/or dark shadows on the downhill side of the feature.

4.4 Image Processing Capabilities

Sophisticated image-processing software is available on all commercial SPMs. Beautiful images can be created by introducing artificial light sources, 3-dimensional rendering (see Figure 4-3), color tables, and curvature enhancement algorithms, by retouching areas of bad data, by filtering environmental noise, and by magnifying or reducing the vertical scale of the image to enhance or minimize surface features of interest. You can flatten an image of a surface of a tiny sphere to look closely at the fine-scale roughness. These are some of the benefits of image-processing software.

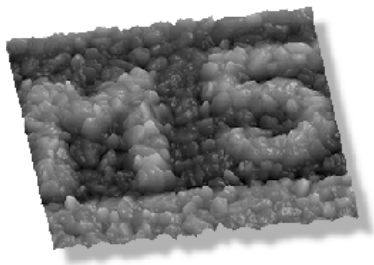

Figure 4-3. 3-D rendered image of a semiconductor surface.

However, when image processing and image enhancement are used carelessly or irresponsibly, data can be misrepresented. The best way to compare the quality of data sets from different SPMs is to compare unprocessed "raw" data in a gray-scale image. As an example of misuse of image processing, Figure 4-4 shows a wholly specious image of a monolayer of an organic film, created entirely from random noise by a carefully crafted filter.

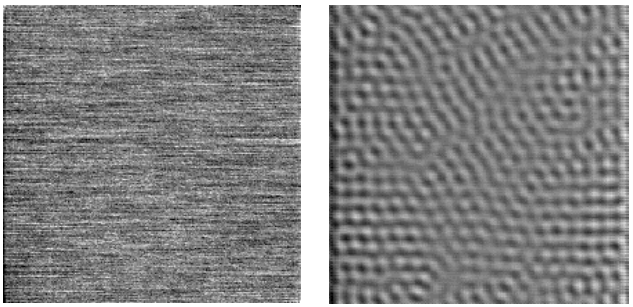

Figure 4-4. AFM image of random noise. Left image is raw data. Right image is a false image, produced by applying a narrow bandpass filter to the raw data.

4.5 Test for Artifacts

Whenever you are suspicious that an image may contain artifacts, follow these steps:

1. *Repeat* the scan to ensure that it looks the same.
2. Change the scan *direction* and take a new image.
3. Change the scan *size* and take an image to ensure that the features scale properly.
4. *Rotate* the sample and take an image to identify tip imaging (see Figure 4-2).
5. Change the scan *speed* and take another image (especially if you see suspicious periodic or quasi-periodic features).

4.6 Further Reading

S.-I. Park, J. Nogami and C. F. Quate, Phys. Rev. B 36, 2863 (1987).

CHAPTER 5
KEY FEATURES OF SPMS

Considerations outside of the scientific realm are likely to be a part of your choice of an SPM. An instrument that is easy to use will have lower operating costs because a highly skilled operator is not required. Minimal training time is desirable in a multi-user facility. Finally, an instrument that is easy to run will be used more—and produce more results. This chapter describes aspects of an SPM that should be evaluated before you purchase an instrument.

5.1 User Interface

Evaluate the complexity of the user interface. It should be laid out in a straightforward, manner with easy-to-use controls. For example, the user interface should have buttons with names that represent commonly performed function such as Approach and Image. After you have seen someone else demonstrate the instrument, ask to operate it yourself. You are then in the best position to evaluate the simplicity of the user interface.

Some SPMs are built upon operating systems that allow multi-tasking. If you can process data while collecting additional data, your throughput will be increased measurably.

5.2 Optical Microscope

All commercial SPMs now include optical microscopes to help monitor the tip-to-sample approach and to select the areas of interest on the sample surface. A good optical microscope speeds up your work because it enables you to position the tip quickly and accurately, exactly where you want to take an SPM image. If you intend to image very rough or oddly shaped samples (for example geological samples, or teeth), or cross sections of any kind that require landing the tip on a narrow edge, a good optical microscope is indispensable. Figure 5-1 shows a real-time video image of a cantilever positioned over an integrated circuit.

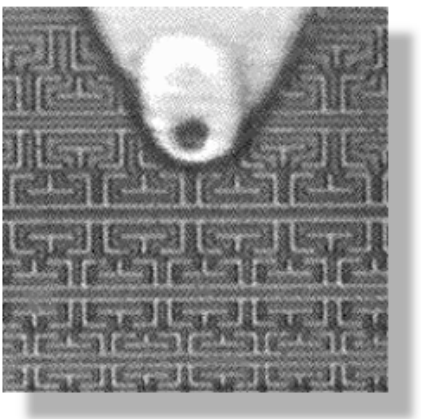

Figure 5-1. Real-time video image of a cantilever positioned over an integrated circuit.

When evaluating the optical microscope, look for the following features:

- optical image clarity
- useful magnification range
- zoom lens
- integrated video camera

Motorized focus and zoom controls are timesavers over manual models, but optical image quality is the most important. The magnification should enable you to navigate rough surfaces and cross sections, to a high magnification, where the field of view allows you to place the tip on micron-sized features. Note that a quoted magnification range is subject to "cheating." If you attach a larger monitor to the same video camera, you end up with higher magnification, but no better resolution. The best way to specify the optical microscope is by field of view or resolution.

5.3 Probe Handling

Under normal operating conditions, an AFM tip should last for a couple of days, so changing the probe should be a straightforward process. However, the chips upon which cantilevers are mounted are very small and can be unwieldy to handle. New designs permit pre-aligned, pre-mounted probes to be changed very quickly, with minimal alignment of the beam-bounce detection system. As with the user interface, you should evaluate how difficult it is to change a probe. Change a probe yourself, instead of watching a highly skilled operator change it.

5.4 System Accessibility

If you intend to perform unique experiments with an SPM, you may be very interested in having access to the software, the electronics, and the mechanics of the system in order to make your own modifications. Investigate the design of the system to see whether it is open enough for your customized work. Consider also the technical strength and availability of the technical support staff at the factory. You may want their advice more often than a user who is happy to operate the machine off-the-shelf.

Notes: